NUCLEAR PHYSICS

Medium effects in λK^+ pair production by 2.83 GeV protons on nuclei

Medium effects in ΛK^+ pair production by 2.83 GeV protons on nuclei *

E. Ya. Paryev[1,2] M. Hartmann[3] Yu. T. Kiselev[2]

[1] Institute for Nuclear Research, Russian Academy of Sciences, Moscow 117312, Russia
[2] Institute for Theoretical and Experimental Physics, Moscow 117218, Russia
[3] Institut für Kernphysik and Jülich Centre for Hadron Physics, Forschungszentrum Jülich, D–52425 Jülich, Germany

Abstract: We study ΛK^+ pair production in the interaction of protons of 2.83 GeV kinetic energy with C, Cu, Ag, and Au target nuclei in the framework of the nuclear spectral function approach for incoherent primary proton–nucleon and secondary pion–nucleon production processes, and processes associated with the creation of intermediate $\Sigma^0 K^+$ pairs. The approach accounts for the initial proton and final Λ hyperon absorption, final K^+ meson distortion in nuclei, target nucleon binding, and Fermi motion, as well as nuclear mean-field potential effects on these processes. We calculate the Λ momentum dependence of the absolute ΛK^+ yield from the target nuclei considered, in the kinematical conditions of the ANKE experiment, performed at COSY, within the different scenarios for the Λ-nucleus effective scalar potential. We show that the above observable is appreciably sensitive to this potential in the low-momentum region. Therefore, direct comparison of the results of our calculations with the data from the ANKE-at-COSY experiment can help to determine the above potential at finite momenta. We also demonstrate that the two-step pion–nucleon production channels dominate in the low-momentum ΛK^+ production in the chosen kinematics and, therefore, they have to be taken into account in the analysis of these data.

Keywords: proton-nucleus reactions, medium effects, hyperon nuclear potential

PACS: 25.40.-k **DOI:** 10.1088/1674-1137/41/12/124108

1 Introduction

The production of strangeness carrying particles has been intensively investigated for a long time in many experiments, using a variety of beams, targets and energies. Strange particles produced in proton-nucleus and nucleus-nucleus reactions interact with the hadronic environment not only by collisions but also by potential interaction, which is expected to lead to a change in the particle properties in matter. Numerous experiments performed during the past two decades were aimed at studying the properties of kaons, antikaons and hyperons in a strongly interacting matter. They were motivated by the theoretically predicted phenomena of the partial restoration of chiral symmetry in hot/dense nuclear matter and the possible existence of an antikaon condensate or the presence of hyperons in the dense core of neutron stars (see Ref. [1] for a recent review).

The in-medium modification effects on the strange meson properties, mass and width, at nuclear saturation density can be described in terms of complex nuclear optical potential. It has been established that the real parts of the K^+ and K^0 repulsive nuclear potentials amount to 20–40 MeV at normal nuclear density $\rho_0 = 0.16$ fm^{-3} [2], while the attractive K^- potential is stronger, although there is no common agreement about its strength so far. The calculations, based on chiral Lagrangians [3,4,5] or on meson-exchange potentials [6], predict a relatively shallow low-energy K^-–nucleus potential with central depth of the order of -50 to -80 MeV. On the other hand, fits to the K^- atomic data in terms of phenomenological density-dependent optical potential or relativistic mean-field calculations [7] lead to a much stronger potential with depth of about -200 MeV at density ρ_0. The reported results of different measurements indicate that the values of the central depth of the potential are spread out over a wide range from -30 to -200 MeV [8]. The recent data for kaon pair production by protons off nuclei obtained by the ANKE Collaboration do not favor a deep antikaon potential [9]. The imaginary part of the nuclear optical potential, which is responsible for the absorption of strange mesons with both open (K^+, K^-) and hidden (ϕ) strangeness during their way out of nuclei, has been also studied by measuring the so-called transparency ratio [10]. These investigations provide information on the in-medium meson width or on the in-medium meson–nucleon cross section.

Essential progress has been made over past decades

Received 28 July 2017, Revised 5 October 2017

∗ Supported by the Ministry of Education and Science of the Russian Federation

in studying the properties of strange mesons in nuclear matter produced in proton–nucleus and nucleus–nucleus collisions at intermediate energies within the different transport models (QMD, IQMD and HSD, GiBUU and LQMD) as well as in investigating in these collisions, by means of kaons, the high-density behavior of the EoS (see Ref. [11] for a review and Ref. [12] for a recent study). It has been shown that the kaon and antikaon mean-field potentials change the structure of the majority of the observables (collective flows, inclusive spectra, their ratios) and make it possible to get good agreement with the available experimental data. Much less attention, however, has been paid to the properties of strange baryons in the surrounding nuclear environment in these collisions at near-threshold beam energies. Recently, Λ and $\Sigma^{+,0,-}$ production in heavy-ion- and proton-induced reactions on nuclei near threshold energies has been investigated within the isospin- and momentum-dependent LQMD transport model [12]. In particular, it was found that the Σ^-/Σ^+ ratio is sensitive to the isospin asymmetric part of the EoS, which is poorly understood up to now. Knowledge of this part is important in astrophysics. The influence of the lambda potential on inclusive Λ creation in pA interactions, however, turned out to be negligible. A large series of results on Λ and Σ hyperon production in proton–nucleus collisions has been compiled in the high energy region from 9 to 400 GeV [13]. Experimental information on their creation at lower proton beam energies is very poor, although the search for medium modification effects here, in particular, in the near-threshold energy domain, looks quite promising. So far, the only experiment here aimed at the study of $\Lambda(1115)$ hyperon production in p+Nb reactions at proton beam energy of 3.5 GeV has been performed by the HADES Collaboration at SIS18/GSI Darmstadt [14]. This kinetic energy corresponds to an excess energy of 0.63 GeV with respect to the threshold of $\Lambda(1115)$ production in NN collisions and to a typical hyperon momentum of about 0.4 GeV/c. However, investigation of possible medium effects has been out of the scope of the performed data analysis, which was directed at studying the most important features of hyperon production. Rich hypernuclear experimental information [15] enables us to study the hyperon–nucleus interaction at (almost) zero hyperon momentum with respect to the nuclear matter.

The in-medium properties of hyperons at finite momentum, density and temperature have become a matter of intense theoretical investigation over past years. Thus, the medium modification of the $\Lambda(1520)$ hyperon has been studied within chiral unitary theory with coupled channels [16]. It was found that at normal nuclear matter density the mass shift of the $\Lambda(1520)$ is small (about 2%), while its in-medium width is more than five times bigger than the free one. The impact of the in-medium $\Lambda(1520)$ width on the hyperon yield from photon– and proton–nucleus reactions has been analyzed in the framework of a collision model based on eikonal approximation in Ref. [17]. The spectral functions for the hyperons have been evaluated in a self-consistent and covariant many-body approach [18]. Attractive mass shifts of about -30 and -40 MeV/c^2 have been predicted for the $\Lambda(1405)$ and $\Sigma(1385)$ hyperons, respectively, at rest at normal nuclear matter density. It has also been found that the $\Lambda(1115)$ hyperon downward mass shift of about -30 MeV/c^2 at this density is quite independent of the three-momentum, but its in-medium width is significantly increased as the hyperon moves with respect to the bulk matter. The predicted mass shift for the $\Sigma(1195)$ is about -22 MeV/c^2 at saturation density. The in-medium properties of the $\Lambda(1115)$, $\Sigma(1195)$ and $\Sigma(1385)$ hyperons have been investigated in the chiral unitary approach [19]. It has been found that $\Lambda(1115)$, $\Sigma(1195)$ and $\Sigma(1385)$ experience an attractive potential of about -50, -40 and -10 MeV, respectively, at normal nuclear matter density and at zero momentum relative to the surrounding nuclear matter. The imaginary parts of the optical potentials of $\Lambda(1115)$ and $\Sigma(1195)$ hyperons are less in absolute magnitude than 10 MeV, while that for the $\Sigma(1385)$ hyperon amounts to -50 MeV at this density and momentum. In contrast to Ref. [18], both the real and imaginary parts of the optical potential for all considered hyperons change significantly in the momentum range from 0 to 600 MeV/c. Recently the momentum dependences of the real and imaginary parts of the single-particle potential of the $\Lambda(1115)$ and $\Sigma(1195)$ hyperons in isospin symmetric and asymmetric nuclear matter have been studied in chiral effective field theory [20]. At saturation density, the real part of the attractive $\Lambda(1115)$ potential is between $-$(24–28) MeV at zero momentum with respect to the nuclear matter, increases with the hyperon momentum and becomes positive (repulsive) at momenta exceeding 400 MeV/c, while a $\Sigma(1195)$ feels a repulsive potential even at zero momentum. Cited in Refs. [18-20], the values of the real part of a $\Lambda(1115)$ potential at saturation density and at zero momentum in the nuclear matter rest frame are somewhat different, but comparable to an empirical value of about -30 MeV deduced from the analysis of binding energies of hypernuclei [15]. On the other hand, the situation with, in particular, the Λ–nuclear potential at finite momenta, is still unclear at present, in spite of a lot theoretical activity in this field. There is currently no experimental information about the momentum dependence of this potential. This information can be deduced from analysis of the experimental data on the production of Λ hyperons in coincidence with K^+ mesons in proton collisions with C, Cu, Ag and Au targets at an initial energy of 2.83 GeV, taken recently by the ANKE Collaboration at the COSY

accelerator. The advantage of such coincident data compared to inclusive data is that fewer individual exclusive elementary Λ production channels need to be accounted for in their interpretation, with the aim of obtaining information on the Λ–nuclear potential, compared to what is involved in the analysis of inclusive data. That makes such interpretations clearer and allows for reduction of the theoretical uncertainties associated with the Λ particle production mechanisms. Moreover, one may hope that such (more differential than the inclusive) coincident data in combination with the available high-energy pA data will allow us to investigate the Λ-nuclear potential.

In this connection, the main goal of the present work is to give predictions for the absolute yields of ΛK^+ pairs from pA collisions in the kinematical conditions of the ANKE experiment, adopting the collision model, based on the nuclear spectral function, for incoherent one-step and two-step ΛK^+ pair creation processes in different scenarios for the lambda–nuclear potential. Direct comparison of these predictions with the expected data from this experiment will allow us to shed light on the Λ potential in a nuclear medium at finite momenta.

2 The model

2.1 Direct ΛK^+ production mechanisms

The direct production of Λ hyperons in coincidence with forward going K^+ mesons in the kinematical conditions of the ANKE experiment in pA collisions at incident energy of 2.83 GeV of our interest can occur in the following pp and pn elementary processes with zero, one and two pions in the final states[1)]

$$\mathrm{p+p\to\Lambda+p+K^+}, \tag{1}$$

$$\begin{aligned}&\mathrm{p+p\to\Lambda+p+\pi^0+K^+},\\ &\mathrm{p+p\to\Lambda+n+\pi^+ +K^+};\end{aligned} \tag{2}$$

$$\begin{aligned}&\mathrm{p+p\to\Lambda+p+\pi^0+\pi^0+K^+},\\ &\mathrm{p+p\to\Lambda+p+\pi^+ +\pi^- +K^+},\\ &\mathrm{p+p\to\Lambda+n+\pi^0+\pi^+ +K^+};\end{aligned} \tag{3}$$

$$\mathrm{p+n\to\Lambda+n+K^+}, \tag{4}$$

$$\begin{aligned}&\mathrm{p+n\to\Lambda+n+\pi^0+K^+},\\ &\mathrm{p+n\to\Lambda+p+\pi^- +K^+};\end{aligned} \tag{5}$$

$$\begin{aligned}&\mathrm{p+n\to\Lambda+n+\pi^0+\pi^0+K^+},\\ &\mathrm{p+n\to\Lambda+n+\pi^+ +\pi^- +K^+},\\ &\mathrm{p+n\to\Lambda+p+\pi^- +\pi^0+K^+}.\end{aligned} \tag{6}$$

Let us now discuss the total cross sections of the reactions (1)–(6), which we will use throughout our calculations of ΛK^+ pair yields in pA collisions. The channel $pp\to\Lambda pK^+$ has been extensively studied experimentally both earlier – mostly at beam energies $\geqslant 2.85$ GeV [21] – and recently – at initial proton energies $\leqslant 2.5$ GeV by the COSY-11, COSY-TOF and ANKE Collaborations (see, for example, [22–29]) as well as very recently–at incident proton energy of 3.5 GeV by the HADES Collaboration [30]. We will use the following parametrization of available experimental data for the total cross section of the $pp\to\Lambda pK^+$ reaction:

$$\sigma_{\mathrm{pp}\to\Lambda\mathrm{pK}^+}(\sqrt{s},\sqrt{s_{\mathrm{th}}})=\begin{cases}\dfrac{A_\Lambda(s-s_{\mathrm{th}})^2}{4m_{\mathrm{p}}^2+B_\Lambda(s-s_{\mathrm{th}})^2} & \text{for } 0.435\ \mathrm{GeV}<\sqrt{s}-\sqrt{s_{\mathrm{th}}}<2.0\ \mathrm{GeV},\\ \dfrac{C_\Lambda\left(\sqrt{s}-\sqrt{s_{\mathrm{th}}}\right)^2}{\left[1+\sqrt{1+(\sqrt{s}-\sqrt{s_{\mathrm{th}}})/D_\Lambda}\right]^2} & \text{for } 0<\sqrt{s}-\sqrt{s_{\mathrm{th}}}\leqslant 0.435\ \mathrm{GeV},\end{cases} \tag{7}$$

where $\sqrt{s}$ is the total pp center-of-mass energy and $\sqrt{s_{\mathrm{th}}}=m_\Lambda+m_{\mathrm{p}}+m_{\mathrm{K}^+}$ is the threshold energy; m_Λ, m_{p} and m_{K^+} are the Λ hyperon, proton and K^+ meson free space masses, respectively; and the constants A_Λ, B_Λ, C_Λ and D_Λ are given as:

$$\begin{aligned}A_\Lambda &= 122.943\ \mu\mathrm{b/GeV^2}, B_\Lambda=2.015/\mathrm{GeV^2},\\ C_\Lambda &= 25740\ \mu\mathrm{b/GeV^2}, D_\Lambda=5.203\cdot 10^{-3}\ \mathrm{GeV}.\end{aligned} \tag{8}$$

This combines the relevant fit from Ref. [31] in the high excess energy region with those given in Refs. [28, 32] in the low energy interval. In Fig. 1 the results of calculations by parametrization (7), (8) for the total cross section $\sigma_{\mathrm{pp}\to\Lambda\mathrm{pK}^+}$ of reaction $pp\to\Lambda pK^+$ are shown as a solid line together with the available data [21–30] on this cross section in the considered range of excess energies. The arrow on this figure indicates the excess energy that corresponds to the beam kinetic energy of 2.83 GeV. This parametrization describes the energy dependence of the cross section $\sigma_{\mathrm{pp}\to\Lambda\mathrm{pK}^+}$ quite well both at low and high

1) Recall that the free threshold energies, e.g., for the processes $pp\to\Lambda pK^+$, $pp\to\Lambda p\pi^0K^+$ and $pp\to\Lambda p\pi^0\pi^0K^+$ amount, respectively, to 1.58, 1.96 and 2.35 GeV. We can neglect at the beam energy of interest the subprocesses $pN\to\Lambda N3\pi K$ with three pions in the final states, due to the proximity of their production thresholds in free pN interactions to this energy. Thus, for instance, the threshold energy of the channel $pp\to\Lambda p3\pi^0K^+$ is 2.77 GeV. This energy is close to the incident proton energy of 2.83 GeV. Hence, the subprocesses $pN\to\Lambda N3\pi K$ are energetically suppressed.

excess energies considered.

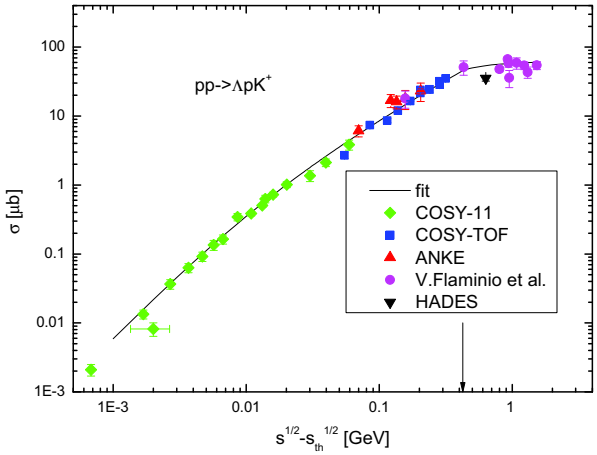

Fig. 1. (color online) Total cross section for $pp\to\Lambda pK^+$ reaction as a function of excess energy. For notation see the text.

Two processes (2) for Λ production together with one pion in pp interactions as well as the process $pp\to\Lambda p\pi^+K^0$ have been measured at proton energies $\geqslant 4.1$ GeV [21], with an exception of two $pp\to\Lambda p\pi^+K^0$ measurements carried out by the ANKE [33] and HADES [34] Collaborations at 2.83 and 3.5 GeV, respectively. The three sets of data, which are available [21] at beam energies $\geqslant 4.1$ GeV for these processes, indicate that they have similar total cross sections (see also Ref. [35]):

$$\sigma_{pp\to\Lambda p\pi^0K^+}\approx\sigma_{pp\to\Lambda n\pi^+K^+}\approx\sigma_{pp\to\Lambda p\pi^+K^0}. \quad (9)$$

We assume that the relations (9) among the cross sections $\sigma_{pp\to\Lambda N\pi K}$ are also valid at lower incident proton energies. For the free total cross section $\sigma_{pp\to\Lambda p\pi^+K^0}$ we have used the following parametrization:

$$\sigma_{pp\to\Lambda p\pi^+K^0}(\sqrt{s},\sqrt{s_{1th}}) = \begin{cases} 1770.5\left(\sqrt{s}-\sqrt{s_{1th}}\right)^{5.62}\ [\mu b] \\ \qquad \text{for } 0<\sqrt{s}-\sqrt{s_{1th}}\leqslant 0.5\ \text{GeV}, \\ 72\left(\sqrt{s}-\sqrt{s_{1th}}\right)\ [\mu b] \\ \qquad \text{for } 0.5\ \text{GeV}<\sqrt{s}-\sqrt{s_{1th}}<3.0\ \text{GeV}, \end{cases} \quad (10)$$

where $\sqrt{s_{1th}}=m_\Lambda+m_p+m_{\pi^+}+m_{K^0}$ is the threshold energy. Here, m_{π^+} and m_{K^0} are the π^+ and K^0 meson free space masses, respectively. A comparison of the results of calculations by (10) (solid line) with the experimental data for the $pp\to\Lambda p\pi^+K^0$ reaction from ANKE [33] (full triangle), from the HADES Collaboration [34] (full square[1)]), and for the data [21] at higher energies (full circles) is shown in Fig. 2. In this figure we also show the predictions from the parametrization (45) (dashed line) employed in the study [35] of kaon creation in heavy–ion collisions. This parametrization significantly overestimates the lowest data point, obtained at 2.83 GeV initial proton kinetic energy.

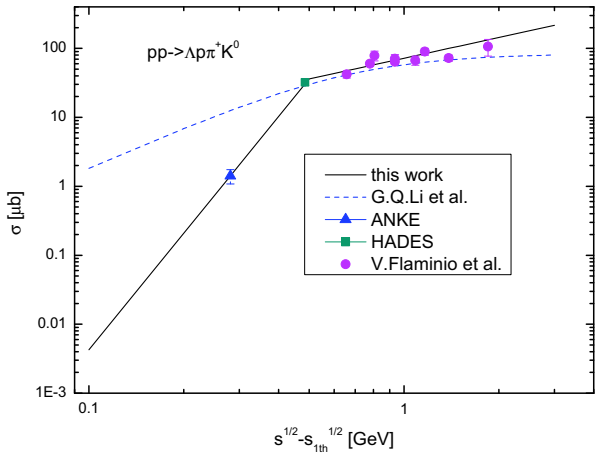

Fig. 2. (color online) Total cross section for $pp\to\Lambda p\pi^+K^0$ reaction as a function of excess energy. For notation see the text.

Now, we consider total cross sections of the reactions (3) with two pions in the final states. The experimental data for these reactions are quite scarce. To date, there exist data for the total cross section $\sigma_{pp\to\Lambda p\pi^+\pi^-K^+}$ of only the process $pp\to\Lambda p\pi^+\pi^-K^+$ [21]. Data also are available for the total cross sections $\sigma_{pp\to\Lambda p\pi^+\pi^0K^0}$ and $\sigma_{pp\to\Lambda n\pi^+\pi^+K^0}$ of the reactions $pp\to\Lambda p\pi^+\pi^0K^0$ and $pp\to\Lambda n\pi^+\pi^+K^0$ respectively [21]. These data were obtained at beam energies beginning with 4.100, 4.641 and 6.045 GeV, respectively, and can be approximately fitted by the following expression suggested in Ref. [35]:

$$\sigma_{pp\to\Lambda p\pi^+\pi^-K^+}\approx\sigma_{pp\to\Lambda p\pi^+\pi^0K^0}\approx\sigma_{pp\to\Lambda n\pi^+\pi^+K^0} \approx \frac{80\left(\sqrt{s}-\sqrt{s_{2th}}\right)^2}{2.25+\left(\sqrt{s}-\sqrt{s_{2th}}\right)^2}\ [\mu b], \quad (11)$$

where $\sqrt{s_{2th}}=m_\Lambda+m_p+2m_{\pi^+}+m_{K^+}$ is the threshold energy. We assume that the other two channels $pp\to\Lambda p\pi^0\pi^0K^+$ and $pp\to\Lambda n\pi^+\pi^0K^+$ have the same cross section [35]. We will also use the parametrization (11) in the present work at incident energy of 2.83 GeV, which is lower than those studied in the compilation in Ref. [21][2)].

1) This data point has been inferred from the measured total cross sections for direct and resonant (via the intermediate Δ^{++}) production of the 4-body final state $\Lambda p\pi^+K^0$ in pp interactions.

2) The relations (11) are in line with the results for the total cross sections for K^0 production channels $pp\to\Lambda p\pi^+\pi^0K^0$ and $pp\to\Lambda n\pi^+\pi^+K^0$ at beam kinetic energy of 3.5 GeV, which can be obtained assuming that these channels go exclusively through the reactions $pp\to\Delta^{++}\Sigma(1385)^0K^0$ and $pp\to\Delta^+\Sigma(1385)^+K^0$ and using formula (2) for the total cross sections of the latter reactions from Ref. [36], in which inclusive K^0 production in pp and pNb interactions was measured with the HADES detector. This gives us confidence that the use of these relations is justified at our beam energy of interest.

Finally, we focus on the total cross sections for Λ production in pn reactions (4)–(6). Up to now, there have been no direct data on Λ production in reaction (4). The relationship between total cross section $\sigma_{\rm pn\to\Lambda nK^+}$ of this reaction and $\sigma_{\rm pp\to\Lambda pK^+}$ for channel (1) can be obtained by the following indirect route. An analysis of the data on the production of K^+ mesons at small angles in proton–proton and proton–deuteron collisions at beam energies of 1.826, 1.920, 2.020 and 2.650 GeV, taken by the ANKE Collaboration [37], gave a value for the ratio of total inclusive K^+ creation cross sections in pn and pp interactions of $\sigma^{\rm K^+}_{\rm pn}/\sigma^{\rm K^+}_{\rm pp}=0.5\pm0.2$ at all four energies investigated. Since the main contribution to the total cross sections of the reactions pn→K^+X and pp→K^+X comes, at least at initial energies ⩽ 2.020 GeV, from the channels pn → ΛnK^+ and pp → ΛpK^+ [38], this means that

$$\sigma_{\rm pn\to\Lambda nK^+}\approx\frac{1}{2}\sigma_{\rm pp\to\Lambda pK^+} \tag{12}$$

at these energies. Further, the Λ hyperon production cross sections in reaction (4) and in channel pn→ΛpK^0 are the same, due to isospin symmetry. There are [21] only five data points for the free total cross section $\sigma_{\rm pn\to\Lambda pK^0}$ of this channel at incident proton kinetic energies of 5.135, 6.124 and 16.088 GeV. Comparing these data with that available [21] for the pp→ΛpK^+ channel at similar energies (5.135, 6.045 and 11.098 GeV), one can easily find that at these energies the pn cross sections $\sigma_{\rm pn\to\Lambda pK^0}$ and $\sigma_{\rm pn\to\Lambda nK^+}$ are about half of the pp cross sections $\sigma_{\rm pp\to\Lambda pK^+}$, namely:

$$\sigma_{\rm pn\to\Lambda pK^0}=\sigma_{\rm pn\to\Lambda nK^+}\approx\frac{1}{2}\sigma_{\rm pp\to\Lambda pK^+}. \tag{13}$$

Accounting for expressions (12) and (13), we will assume that

$$\sigma_{\rm pn\to\Lambda nK^+}(\sqrt{s})\approx\frac{1}{2}\sigma_{\rm pp\to\Lambda pK^+}(\sqrt{s},\sqrt{s_{\rm th}}) \tag{14}$$

also at all center-of-mass energies $\sqrt{s}$, accessible in calculation of ΛK^+ production in pA reactions at our beam energy of interest, 2.83 GeV, with allowance for the Fermi motion of intranuclear nucleons[1)]. The only set of data is available for Λ hyperon production together with one pion in pn collisions. It was obtained for pn→Λp$\pi^-$$K^+$ reaction at incident energies starting from 5.135 GeV [21]. The set indicates the total cross section $\sigma_{\rm pn\to\Lambda p\pi^-K^+}$ of this reaction, which is about half of those in Eqs. (9), (10) for pp processes (2) (cf. Ref. [35]). In line with Ref. [35], we will assume that the other pn channel pn → Λn$\pi^0$$K^+$ from Eq. (5) has the same cross section as the pn→Λp$\pi^-$$K^+$ reaction. Under the above assumptions, we have:

$$\begin{aligned}\sigma_{\rm pn\to\Lambda n\pi^0K^+}(\sqrt{s}) &\approx \sigma_{\rm pn\to\Lambda p\pi^-K^+}(\sqrt{s})\\ &\approx \frac{1}{2}\sigma_{\rm pp\to\Lambda p\pi^+K^0}(\sqrt{s},\sqrt{s_{\rm 1th}}).\end{aligned} \tag{15}$$

These relations (15) will be used in our calculations of ΛK^+ pair yields from pA collisions at all accessible values of the center-of-mass energy $\sqrt{s}$. The only set of data there is at present for Λ hyperon production together with two pions in pn interactions. It was taken for the pn → Λp$\pi^+$$\pi^-$$K^0$ reaction at beam energies of 5.135, 6.124 and 16.088 GeV [21]. The set indicates that the total cross section $\sigma_{\rm pn\to\Lambda p\pi^+\pi^-K^0}$ of this reaction is about half of those (11) for the corresponding pp channels (3) (cf. Ref. [35]). As in Ref. [35], we will assume that all three pn processes (6) have the same cross section as the pn → Λp$\pi^+$$\pi^-$$K^0$ reaction. In this context, one gets:

$$\begin{aligned}\sigma_{\rm pn\to\Lambda n\pi^0\pi^0K^+}(\sqrt{s}) &\approx \sigma_{\rm pn\to\Lambda n\pi^+\pi^-K^+}(\sqrt{s})\\ &\approx \sigma_{\rm pn\to\Lambda p\pi^-\pi^0K^+}(\sqrt{s})\\ &\approx \sigma_{\rm pn\to\Lambda p\pi^+\pi^-K^0}(\sqrt{s})\\ &\approx \frac{1}{2}\sigma_{\rm pp\to\Lambda p\pi^+\pi^-K^+}(\sqrt{s},\sqrt{s_{\rm 2th}}).\end{aligned} \tag{16}$$

We will use Eq. (16) at all collision energies of interest. It is worth noting that, as follows from Eqs. (7)–(16), the ratios of Λ production cross sections in the pp and pn processes (2), (3) and (5), (6) with one as well as with two pions in the final states to those of Λ creation channels (1) and (4) with zero outgoing pions are about of 1/9 at kinetic beam energy of 2.83 GeV of interest. This means that the main contribution to Λ production in pA reactions, even at this high incident energy, comes from the 3-body primary channels (1) and (4).

For numerical simplicity, in the following calculations we will include the medium modification of the final nucleon, kaon and Λ hyperon, participating in the production processes (1)–(6), by using their average in-medium masses $<m_h^*>$ instead of their local effective masses $m_h^*(r)$ in the in-medium cross sections of these processes, with $<m_h^*>$ defined in line with Refs. [31, 42] as:

$$<m_h^*>=m_h+U_h\frac{<\rho_N>}{\rho_0}. \tag{17}$$

Here, m_h is the hadron free space mass, U_h is the value of its effective scalar nuclear potential at saturation density ρ_0[2)], and $<\rho_N>$ is the average nucleon density, which was calculated separately for each target nucleus considered. Our calculations show that for target nuclei C, Cu, Ag and Au the ratio $<\rho_N>/\rho_0$ is approximately equal to 0.55, 0.65, 0.72 and 0.77, respectively.

1) Theoretical estimates of the ratio $\sigma_{\rm pn\to\Lambda nK^+}/\sigma_{\rm pp\to\Lambda pK^+}$, obtained on the basis of the meson-exchange models [39–41], are around 2 [39], 3 [40] or range from 0.25 to 10 [32, 41], which is inconsistent with experimental results (12) and (13).

2) This potential is not the usual Lorentz scalar potential, but contains both the Lorentz scalar and Lorentz vector potentials, like Eq. (23) below.

The above values will be used throughout the following study. We assume that pions do not change their properties in the nuclear medium at densities of ordinary nuclei [43]. To match smoothly in-medium Λ hyperon production thresholds in pp collisions to those in pn interactions, we also neglect the influence of the Coulomb potentials on the final charged hadrons (protons, pions and kaons), participating in the elementary reactions (1)–(6). In addition, these potentials, as expected, have a minor role in the Λ dynamics at our initial proton energy of interest. The total energy E'_h of the hadron inside the nuclear medium can be expressed through its average effective mass $< m^*_h >$ defined above and its in-medium momentum $\mathbf{p}'_h$ as in the free particle case, namely:

$$E'_h = \sqrt{(<m^*_h>)^2 + (\boldsymbol{p}'_h)^2}. \tag{18}$$

The momentum $\boldsymbol{p}'_h$ is related to the vacuum momentum $\boldsymbol{p}_h$ by the following expression:

$$E'_h = \sqrt{(<m^*_h>)^2 + (\boldsymbol{p}'_h)^2} = \sqrt{m_h^2 + \boldsymbol{p}_h^2} = E_h, \tag{19}$$

where E_h is the hadron vacuum total energy. In the subsequent study for the K^+ mass shift U_{K^+} we will always employ the following option: $U_{K^+} = 22$ MeV [44]. The same option will be adopted for the K^0 mass shift U_{K^0} [1]. The relation between the effective scalar nucleon potential U_N, entering into Eq. (17), and the corresponding Schrödinger equivalent potential $V_{NA}^{\rm SEP}$ (or the so-called single-particle or mean-field potential) at the normal nuclear matter density is given by

$$U_N = \frac{\sqrt{m_N^2 + {p'_N}^2}}{m_N} V_{NA}^{\rm SEP}. \tag{20}$$

As shown in our calculations, the vacuum momenta of the outgoing nucleons in reactions (1)–(6) are around p_N=0.6 GeV/c in the kinematics of the ANKE experiment. Assuming that $p'_N \approx p_N$ [2] and using $V_{NA}^{\rm SEP} \approx 0$ MeV at this in-medium nucleon momentum, corresponding to a kinetic energy of 0.18 GeV [46], we can readily obtain that $U_N \approx 0$ MeV. We will employ this potential throughout our present work.

Let us now specify the effective scalar mean-field Λ hyperon potential U_Λ in Eq. (17). A nuclear mean-field potential acting on the bound in the nucleus low-momentum Λ hyperon has been extracted from the properties of hypernuclei [47]. This potential has also been investigated in the framework of relativistic mean-field theory [48, 49]. It was found from these studies that the well depth for a Λ particle embedded in nuclear matter is in the vicinity of 30 MeV. The kinetic energy dependence of the Λ–nucleus mean-field potential for Λ hyperons colliding with a nucleus was evaluated in Ref. [50] within the G-matrix theory over the Λ kinetic energy range of 0–70 MeV (or over the Λ momentum interval of 0–0.4 GeV/c). The momentum dependence of this potential was studied in Ref. [51] within the framework of the relativistic Brueckner–Hartree–Fock theory, employing two kinds of YN phenomenological potentials – Juelich 94a and Juelich 05 – constructed with the meson-exchange model by the Juelich group, at the same Λ momenta as in Ref. [50], and as in Ref. [19] within the chiral unitary coupled-channel approach for Λ momenta ranging up to 0.6 GeV/c. In both Refs. [51] and [19], similar behavior was found for the Λ potential at normal nuclear matter density: it is attractive and increases monotonically with the growth of Λ momentum. The Λ single-particle potential in isospin symmetric and asymmetric nuclear matter at finite momenta up to 0.6 GeV/c has been also investigated recently in Ref. [20], in the framework of the Brueckner approach using the ΛN potential derived from $SU(3)$ chiral effective field theory at next-to-leading order, as was already noted above. Contrary to the results from Refs. [51, 19], this potential turns from attractive to repulsive at about 0.4 GeV/c momentum in isospin symmetric nuclear medium at saturation density. Moreover, the Λ single-particle potential in symmetric nuclear matter has been calculated in Ref. [52] within the $SU(6)$ quark model at various nuclear densities as a function of the momentum in the range of about 0–1.4 GeV/c. An essential difference between this potential and that from Ref. [20] is that it turns to repulsion at fairly high momenta, around 1.1 GeV/c. Recently, the momentum and density dependences of the Λ hyperon single-particle potential in nuclear medium was calculated starting from QCD on the lattice [53]. The reported results are compatible with those obtained within other approaches. Since the accessible range of the Λ hyperon momenta in the ANKE experiment is about 0.4–3 GeV/c, it is helpful to also estimate the Λ mean-field potential, needed for our present study, for such high Λ momenta. We will rely on the constituent quark model, which has been employed in Ref. [54] to derive the density dependence of the low-momentum Λ–nucleus potential, and will proceed analogously with the aim of obtaining its momentum dependence at saturation density ρ_0. In this model, the Λ mean-field scalar $U_{S\Lambda}$ and vector $U_{V\Lambda}$ potentials are about 2/3 of U_{SN} and U_{VN} of a nucleon when in-medium nucleon and Λ hyperon velocities v'_N and v'_Λ relative to the nuclear matter are equal to

1) This is not true for heavy nuclei like Au where there the difference between numbers of protons and neutrons is large due to the ρ meson, which induces different mean-field potentials for K^+ and K^0 mesons when they are embedded in asymmetric nuclear matter. However, this effect is expected to be negligible for the present approach in which the nuclear densities $\rho_N \leqslant \rho_0$ are considered [45]. Isospin effects lead also to only small corrections to the K^+ mass shift U_{K^+} when going from a C to an Au target nucleus. They are within 5%, as our estimate, based on the K^+p and K^+n scattering lengths, shows.

2) This point has been numerically checked by employing Eq. (19).

each other, i.e.,

$$U_{S\Lambda}(v'_\Lambda,\rho_N) = \frac{2}{3}U_{SN}(v'_N,\rho_N),$$
$$U_{V\Lambda}(v'_\Lambda,\rho_N) = \frac{2}{3}U_{VN}(v'_N,\rho_N);\ \ v'_N=v'_\Lambda. \quad (21)$$

The latter term in Eq. (21) corresponds, as is easy to see, to the following relation between the respective in-medium nucleon momentum p'_N and the Λ momentum p'_Λ:

$$p'_N=\frac{<m^*_N>}{<m^*_\Lambda>}p'_\Lambda. \quad (22)$$

However, for reasons of numerical simplicity, calculating the Λ–nucleus mean-field potential, we will use the free space nucleon and Λ hyperon masses m_N and m_Λ in Eq. (22) instead of their average in-medium masses $<m^*_N>$ and $<m^*_\Lambda>$. Then, this potential $V^{\rm SEP}_{\Lambda A}$ can be defined as [54][1)]:

$$V^{\rm SEP}_{\Lambda A}(p'_\Lambda,\rho_N) = \sqrt{[m_\Lambda+U_{S\Lambda}(p'_\Lambda,\rho_N)]^2+{p'_\Lambda}^2} + U_{V\Lambda}(p'_\Lambda,\rho_N)-\sqrt{m^2_\Lambda+{p'_\Lambda}^2}. \quad (23)$$

Adopting the momentum-dependent parametrization for the nucleon scalar and vector potentials at saturation density ρ_0 from Ref. [46],

$$U_{SN}(p'_N,\rho_0)=-\frac{494.2272}{1+0.3426\sqrt{p'_N/p_F}}\ {\rm MeV}, \quad (24)$$

$$U_{VN}(p'_N,\rho_0)=\frac{420.5226}{1+0.4585\sqrt{p'_N/p_F}}\ {\rm MeV} \quad (25)$$

(where $p_F = 1.35$ fm^{-1} $=0.2673$ GeV/c) and using Eqs. (21)–(23), we calculated the momentum dependence of potential $V^{\rm SEP}_{\Lambda A}$ at density ρ_0[2)]. It is shown by the dashed curve in Fig. 3. We have also made an adjustment by multiplying the vector Λ hyperon potential by a factor of 1.068, to get a value for the potential $V^{\rm SEP}_{\Lambda A}$ at zero momentum consistent with the experimental value of $-(32\pm2)$ MeV (full circle in figure 3), extracted from the data on binding energies of Λ single-particle states in nuclei [47]. The potential adjusted in this way is presented by the solid curve in Fig. 3. In this case the Λ–nucleus potential is attractive for momenta $\leqslant 0.7$ GeV/c, whereas it becomes repulsive for higher momenta and reaches the value ≈ 70 MeV at Λ momentum of 3 GeV/c.

As follows from Figs. 5–10, the coincident ΛK^+ yield is appreciably sensitive to the lambda potential at vacuum momenta around $p_\Lambda = 1$ GeV/c, where the secondary pion–nucleon ΛK^+ production channels (49) and (50) considered below are dominant. Assuming that, as in the nucleon case above, $p'_\Lambda \approx p_\Lambda$ and using the results shown in Fig. 3, we find that $V^{\rm SEP}_{\Lambda A} \approx 20$ MeV for this in-medium lambda momentum. Then, taking into account that the relation between the effective scalar hyperon potential U_Λ, in Eq. (17), and the corresponding Schrödinger equivalent potential $V^{\rm SEP}_{\Lambda A}$ at normal nuclear matter density is given by the relation analogous to Eq. (20) for nucleons, we can readily obtain that $U_\Lambda\approx30$ MeV at the above Λ momentum. Since the ΛK^+ yield from the direct ΛK^+ production mechanisms considered is concentrated mainly at Λ momenta around $p_\Lambda \approx 2.6$ GeV/c, for which it reacts weakly on the Λ–nuclear potential, as follows from Figs. 7–10, we will adopt the value $U_\Lambda\approx30$ MeV in our calculations of this yield. However, in reality it is still unclear which Λ–nucleus potential is the correct one for such high Λ momenta (cf., for instance, results from Refs. [20] and [52]). Therefore, to extend the range of applicability of our model, we will also calculate the Λ production cross sections off nuclei in scenarios with possible Λ mass shift (or effective scalar potential) U_Λ ranging from -30 MeV to 60 MeV.

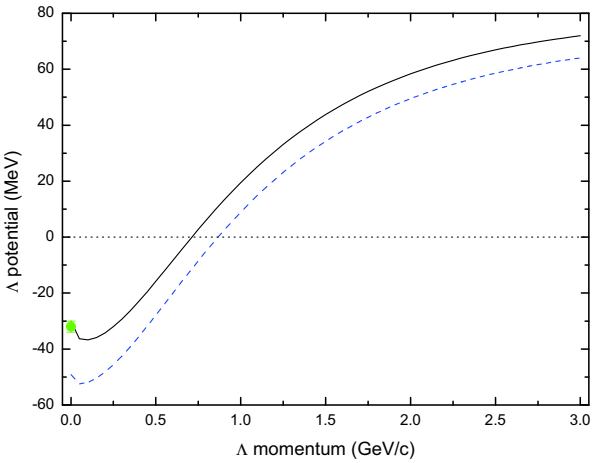

Fig. 3. (color online) Schrödinger equivalent Λ hyperon potential at density ρ_0 as a function of Λ momentum relative to the nuclear matter at rest calculated on the basis of Eq. (23), without and with rescaling its vector potential by a factor of 1.068 (dashed and solid lines, respectively).

Accounting for the distortions of the initial proton and final Λ hyperon and kaon as well as the fact that in the ANKE experiment the latter were detected in the forward polar angular domains $0^\circ \leqslant \theta_\Lambda \leqslant 6^\circ$ and $0^\circ\leqslant\theta_{\rm K^+}\leqslant12^\circ$, respectively, and using the results given in Refs. [55–58], we can represent the differential cross section for the production on nuclei of Λ hyperons with the

1) The space-like component of the Λ vector self-energy is ignored here.

2) Adopting the momentum-dependent parametrization for the nucleon scalar and vector potentials at different nuclear densities from Ref. [46] and using Eq. (23), it is easy to also calculate the density dependence of potential $V^{\rm SEP}_{\Lambda A}$ at different lambda momenta. However, this is beyond the scope of the present work, since here our attention is focussed mainly on the Λ in-medium properties at saturation density ρ_0.

vacuum momentum $\boldsymbol{p}_\Lambda$ in coincidence with K^+ mesons with the vacuum momentum $\boldsymbol{p}_{K^+}$ in the primary proton-induced reaction channels (1)–(6) as follows:

$$\frac{\mathrm{d}\sigma^{(\mathrm{prim})}_{\mathrm{pA}\to\Lambda\mathrm{K}^+\mathrm{X}}(\boldsymbol{p}_0,\boldsymbol{p}_\Lambda,\boldsymbol{p}_{\mathrm{K}^+})}{\mathrm{d}\boldsymbol{p}_\Lambda\mathrm{d}\boldsymbol{p}_{\mathrm{K}^+}}=I_{\mathrm{K}^+\Lambda}[A]\left[\frac{Z}{A}\left\langle\frac{\mathrm{d}\sigma_{\mathrm{pp}\to\Lambda\mathrm{K}^+\mathrm{X}}(\boldsymbol{p}'_0,\boldsymbol{p}'_\Lambda,\boldsymbol{p}'_{\mathrm{K}^+})}{\mathrm{d}\boldsymbol{p}'_\Lambda\mathrm{d}\boldsymbol{p}'_{\mathrm{K}^+}}\right\rangle_A+\frac{N}{A}\left\langle\frac{\mathrm{d}\sigma_{\mathrm{pn}\to\Lambda\mathrm{K}^+\mathrm{X}}(\boldsymbol{p}'_0,\boldsymbol{p}'_\Lambda,\boldsymbol{p}'_{\mathrm{K}^+})}{\mathrm{d}\boldsymbol{p}'_\Lambda\mathrm{d}\boldsymbol{p}'_{\mathrm{K}^+}}\right\rangle_A\right]\frac{\mathrm{d}\boldsymbol{p}'_\Lambda}{\mathrm{d}\boldsymbol{p}_\Lambda}\frac{\mathrm{d}\boldsymbol{p}'_{\mathrm{K}^+}}{\mathrm{d}\boldsymbol{p}_{\mathrm{K}^+}},\tag{26}$$

where

$$I_{\mathrm{K}^+\Lambda}[A]=2\pi A\int_0^R r_\perp\mathrm{d}r_\perp\int_{-\sqrt{R^2-r_\perp^2}}^{\sqrt{R^2-r_\perp^2}}\mathrm{d}z\rho(\sqrt{r_\perp^2+z^2})\exp\left[-\sigma^{\mathrm{in}}_{pN}A\int_{-\sqrt{R^2-r_\perp^2}}^{z}\rho(\sqrt{r_\perp^2+x^2})\mathrm{d}x-\sigma^{\mathrm{tot}}_{\mathrm{K}^+\mathrm{N}}A\int_{z}^{\sqrt{R^2-r_\perp^2}}\rho(\sqrt{r_\perp^2+x^2})\mathrm{d}x\right]$$
$$\times\exp\left[-\sigma^{\mathrm{tot}}_{\Lambda N}(p'_\Lambda)A\int_{z}^{\sqrt{R^2-r_\perp^2}}\rho(\sqrt{r_\perp^2+x^2})dx\right],\tag{27}$$

$$\left\langle\frac{\mathrm{d}\sigma_{\mathrm{pN}\to\Lambda\mathrm{K}^+\mathrm{X}}(\boldsymbol{p}'_0,\boldsymbol{p}'_\Lambda,\boldsymbol{p}'_{\mathrm{K}^+})}{\mathrm{d}\boldsymbol{p}'_\Lambda\mathrm{d}\boldsymbol{p}'_{\mathrm{K}^+}}\right\rangle_A=\int\int P_A(\boldsymbol{p}_t,E)\mathrm{d}\boldsymbol{p}_t\mathrm{d}E\left\{\frac{\mathrm{d}\sigma_{\mathrm{pN}\to\Lambda\mathrm{K}^+\mathrm{X}}[\sqrt{s},<m^*_{\mathrm{K}^+}>,<m^*_N>,<m^*_\Lambda>,\boldsymbol{p}'_\Lambda,\boldsymbol{p}'_{\mathrm{K}^+}]}{\mathrm{d}\boldsymbol{p}'_\Lambda\mathrm{d}\boldsymbol{p}'_{\mathrm{K}^+}}\right\},\tag{28}$$

and

$$p'_\Lambda=\sqrt{E^2_\Lambda-(<m^*_\Lambda>)^2},\ E_\Lambda=\sqrt{m^2_\Lambda+\boldsymbol{p}^2_\Lambda}.\tag{29}$$

Here, $\mathrm{d}\sigma_{\mathrm{pN}\to\Lambda\mathrm{K}^+\mathrm{X}}[\sqrt{s},<m^*_{\mathrm{K}^+}>,<m^*_N>,<m^*_\Lambda>,\boldsymbol{p}'_\Lambda,\boldsymbol{p}'_{\mathrm{K}^+}]/\mathrm{d}\boldsymbol{p}'_\Lambda\mathrm{d}\boldsymbol{p}'_{\mathrm{K}^+}$ are the "in-medium" differential cross sections for the production of Λ hyperons and K^+ mesons with the in-medium momenta $\boldsymbol{p}'_\Lambda$ and $\boldsymbol{p}'_{\mathrm{K}^+}$, correspondingly, in reactions (1)–(3) ($N=p$) and in (4)–(6) ($N=n$) at the pN center-of-mass energy $\sqrt{s}$; $\rho(r)$ and $P_A(\boldsymbol{p}_t,E)$ are the local nucleon density and the spectral function of the target nucleus A normalized to unity, respectively; $\boldsymbol{p}_t$ and E are the internal momentum and binding energy of the struck target nucleon just before the collision, respectively; $\sigma^{\mathrm{in}}_{pN}$ and $\sigma^{\mathrm{tot}}_{\mathrm{K}^+\mathrm{N}}$, $\sigma^{\mathrm{tot}}_{\Lambda N}$ are the inelastic and total cross sections of the pN and K^+N, ΛN interactions respectively; Z and N are the numbers of protons and neutrons respectively in the target nucleus ($A=Z+N$), and R is its radius; and $\boldsymbol{p}_0$ and $\boldsymbol{p}'_0$ are the momenta of the initial proton outside and inside the target nucleus respectively. They are linked by the equation [57]:

$$\boldsymbol{p}'_0=\boldsymbol{p}_0-\Delta\boldsymbol{p},\ \Delta\boldsymbol{p}=\frac{E_0V_0}{p_0}\frac{\boldsymbol{p}_0}{|\boldsymbol{p}_0|},\tag{30}$$

where E_0 and V_0 are the total energy of the initial proton outside the nucleus and the nuclear optical potential that this proton feels in the interior of the nucleus ($V_0\approx40$ MeV) respectively. The expression for s is given by the formula [57]:

$$s=(E'_0+E_t)^2-(\boldsymbol{p}'_0+\boldsymbol{p}_t)^2,\tag{31}$$

where

$$E'_0=E_0-\frac{\Delta\boldsymbol{p}^2}{2M_A},\tag{32}$$

$$E_t=M_A-\sqrt{(-\boldsymbol{p}_t)^2+(M_A-m_N+E)^2}.\tag{33}$$

Here, M_A is the mass of the target nucleus.

For the ΛK^+ production calculations in the cases of the ^{12}C, ^{63}Cu, ^{108}Ag, and ^{197}Au target nuclei reported here, we have employed for the nuclear density $\rho(\boldsymbol{r})$, respectively, the harmonic oscillator and the Woods-Saxon distributions:

$$\rho(\boldsymbol{r})=\rho_N(\boldsymbol{r})/A=\frac{(b/\pi)^{3/2}}{A/4}\left\{1+\left[\frac{A-4}{6}\right]br^2\right\}\exp(-br^2),\tag{34}$$

$$\rho(\boldsymbol{r})=\rho_0\left[1+\exp\left(\frac{r-R_{1/2}}{a}\right)\right]^{-1}\tag{35}$$

with $b=0.355$ fm^{-2} and $R_{1/2}=4.20$ fm for ^{63}Cu, $R_{1/2}=5.505$ fm for ^{108}Ag, $R_{1/2}=6.825$ fm for ^{197}Au, and $a=0.55$ fm for all nuclei [55, 59]. The nuclear spectral function $P_A(\boldsymbol{p}_t,E)$ (which represents the probability of finding a nucleon with momentum $\boldsymbol{p}_t$ and removal energy E in the nucleus) for the ^{12}C target nucleus was taken from Ref. [60]. The single-particle part of this function for the ^{63}Cu, ^{108}Ag and ^{197}Au target nuclei was assumed to be the same as that for ^{208}Pb [44]. The latter was taken from Ref. [61]. The correlated part of the nuclear spectral function for these target nuclei was borrowed from Ref. [60]. Using the total cross sections $\sigma^{\mathrm{tot}}_{K^+N}$ and $\sigma^{\mathrm{tot}}_{\Lambda N}$ in Eq. (27), we assume that if a kaon or a Λ hyperon undergoes a quasi-elastic collision with the target nucleon, it will not fall in the ANKE acceptance window.

Taking into account the above arguments that the main contribution to the primary ΛK^+ production in pA collisions at the considered beam energy of 2.83 GeV will come from the three-body direct processes (1) and (4), we describe the in-medium differential cross sections $\mathrm{d}\sigma_{\mathrm{pN}\to\Lambda\mathrm{K}^+\mathrm{X}}[\sqrt{s},<m^*_{\mathrm{K}^+}>,<m^*_N>,<m^*_\Lambda>$

$,\boldsymbol{p}'_\Lambda,\boldsymbol{p}'_{\rm K^+}]/{\rm d}\boldsymbol{p}'_\Lambda{\rm d}\boldsymbol{p}'_{\rm K^+}$ according to the three-body phase space. Following Ref. [57], we obtain:

$$\begin{aligned}&\frac{{\rm d}\sigma_{\rm pN\to\Lambda K^+X}[\sqrt{s},<m^*_{\rm K^+}>,<m^*_N>,<m^*_\Lambda>,\boldsymbol{p}'_\Lambda,\boldsymbol{p}'_{\rm K^+}]}{{\rm d}\boldsymbol{p}'_\Lambda{\rm d}\boldsymbol{p}'_{\rm K^+}}\\=&\frac{1}{8E'_\Lambda E'_{\rm K^+}}\frac{\sigma_{\rm pN\to\Lambda K^+X}(\sqrt{s},\sqrt{s^*_{\rm th}},\sqrt{s^*_{\rm 1th}},\sqrt{s^*_{\rm 2th}})}{I_3(s,<m^*_{\rm K^+}>,<m^*_N>,<m^*_\Lambda>)}\\&\times\frac{1}{(\omega+E_t)}\delta\Big(\omega+E_t-\sqrt{(<m^*_N>)^2+(\boldsymbol{Q}+\boldsymbol{p}_t)^2}\Big),\end{aligned}\tag{36}$$

where

$$\omega=E'_0-E'_\Lambda-E'_{\rm K^+},\ \boldsymbol{Q}=\boldsymbol{p}'_0-\boldsymbol{p}'_\Lambda-\boldsymbol{p}'_{\rm K^+}\tag{37}$$

and the quantity I_3 is defined as [57]:

$$\begin{aligned}&I_3(s,<m^*_{\rm K^+}>,<m^*_N>,<m^*_\Lambda>)\\=&\Big(\frac{\pi}{2}\Big)^2\int\limits_{(<m^*_{\rm K^+}>+<m^*_N>)^2}^{(\sqrt{s}-<m^*_\Lambda>)^2}\frac{\lambda[x,(<m^*_{\rm K^+}>)^2,(<m^*_N>)^2]}{x}\\&\times\frac{\lambda[s,x,(<m^*_\Lambda>)^2]}{s}{\rm d}x,\end{aligned}\tag{38}$$

$$\lambda[x,y,z]=\sqrt{\big[x-(\sqrt{y}+\sqrt{z})^2\big]\big[x-(\sqrt{y}-\sqrt{z})^2\big]}.\tag{39}$$

Here, $\sigma_{\rm pN\to\Lambda K^+X}(\sqrt{s},\sqrt{s^*_{\rm th}},\sqrt{s^*_{\rm 1th}},\sqrt{s^*_{\rm 2th}})$ are the "in-medium" total cross sections for the $\Lambda{\rm K}^+$ production in reactions (1)–(3) ($N=p$) as well as in (4)–(6) ($N=n$), with the threshold energies $\sqrt{s^*_{\rm th}}=<m^*_\Lambda>+<m^*_p>+<m^*_{\rm K^+}>$, $\sqrt{s^*_{\rm 1th}}=<m^*_\Lambda>+<m^*_p>+m_{\pi^+}+<m^*_{\rm K^0}>$ and $\sqrt{s^*_{\rm 2th}}=<m^*_\Lambda>+<m^*_p>+2m_{\pi^+}+<m^*_{\rm K^+}>$. As in Ref. [58], we assume that these cross sections are equivalent to the vacuum cross sections $\sigma_{\rm pN\to\Lambda K^+X}(\sqrt{s},\sqrt{s_{\rm th}},\sqrt{s_{\rm 1th}},\sqrt{s_{\rm 2th}})$ in which the free threshold energies $\sqrt{s_{\rm th}}$, $\sqrt{s_{\rm 1th}}$ and $\sqrt{s_{\rm 2th}}$ are replaced by the in-medium threshold energies $\sqrt{s^*_{\rm th}}$, $\sqrt{s^*_{\rm 1th}}$ and $\sqrt{s^*_{\rm 2th}}$. Due to the above considerations, the vacuum cross sections $\sigma_{pp\to\Lambda K^+X}(\sqrt{s},\sqrt{s_{\rm th}},\sqrt{s_{\rm 1th}},\sqrt{s_{\rm 2th}})$ and $\sigma_{\rm pn\to\Lambda K^+X}(\sqrt{s},\sqrt{s_{\rm th}},\sqrt{s_{\rm 1th}},\sqrt{s_{\rm 2th}})$ can be defined as:

$$\begin{aligned}&\sigma_{\rm pp\to\Lambda K^+X}(\sqrt{s},\sqrt{s_{\rm th}},\sqrt{s_{\rm 1th}},\sqrt{s_{\rm 2th}})\\=&\sigma_{\rm pp\to\Lambda pK^+}(\sqrt{s},\sqrt{s_{\rm th}})+2\sigma_{\rm pp\to\Lambda p\pi^+K^0}(\sqrt{s},\sqrt{s_{\rm 1th}})\\&+3\sigma_{\rm pp\to\Lambda p\pi^+\pi^-K^+}(\sqrt{s},\sqrt{s_{\rm 2th}}),\end{aligned}\tag{40}$$

$$\begin{aligned}&\sigma_{\rm pn\to\Lambda K^+X}(\sqrt{s},\sqrt{s_{\rm th}},\sqrt{s_{\rm 1th}},\sqrt{s_{\rm 2th}})\\=&\frac{1}{2}\sigma_{\rm pp\to\Lambda pK^+}(\sqrt{s},\sqrt{s_{\rm th}})+\sigma_{\rm pp\to\Lambda p\pi^+K^0}(\sqrt{s},\sqrt{s_{\rm 1th}})\\&+\frac{3}{2}\sigma_{\rm pp\to\Lambda p\pi^+\pi^-K^+}(\sqrt{s},\sqrt{s_{\rm 2th}})\\=&\frac{1}{2}\sigma_{\rm pp\to\Lambda K^+X}(\sqrt{s},\sqrt{s_{\rm th}},\sqrt{s_{\rm 1th}},\sqrt{s_{\rm 2th}}).\end{aligned}\tag{41}$$

We now specify the cross sections $\sigma^{\rm in}_{\rm pN}$, $\sigma^{\rm tot}_{\rm K^+N}$ and $\sigma^{\rm tot}_{\Lambda\rm N}$, in Eq. (27). We use $\sigma^{\rm in}_{\rm pN}=30$ mb for the incident proton energy and $\sigma^{\rm tot}_{\rm K^+N}=12$ mb for all kaon momenta involved in our calculations [58]. Due to the isospin symmetry, the total cross sections $\sigma^{\rm tot}_{\Lambda\rm p}$ and $\sigma^{\rm tot}_{\Lambda\rm n}$ of the free Λp and Λn interactions are the same and we denote them as $\sigma^{\rm tot}_{\Lambda\rm N}$. At Λ momenta of a few GeV/c of interest the cross section $\sigma^{\rm tot}_{\Lambda\rm p}$ is entirely exhausted, as our calculations show, by the total cross sections $\sigma_{\Lambda\rm p\to\Lambda p}$ and $\sigma_{\Lambda\rm p\to\Sigma^0 p}$, $\sigma_{\Lambda\rm p\to\Sigma^+ n}$ of elastic $\Lambda{\rm p}\to\Lambda{\rm p}$ and inelastic $\Lambda{\rm p}\to\Sigma^0{\rm p}$, $\Lambda{\rm p}\to\Sigma^+{\rm n}$ processes. The isospin considerations show that $\sigma_{\Lambda\rm p\to\Sigma^+ n}=2\sigma_{\Lambda\rm p\to\Sigma^0 p}$. With these, we have:

$$\sigma^{\rm tot}_{\Lambda\rm N}=\sigma^{\rm tot}_{\Lambda\rm p}=\sigma_{\Lambda\rm p\to\Lambda p}+3\sigma_{\Lambda\rm p\to\Sigma^0 p}.\tag{42}$$

For the free lambda-proton total cross sections $\sigma_{\Lambda\rm p\to\Lambda p}$ and $\sigma_{\Lambda\rm p\to\Sigma^0 p}$ as functions of the laboratory Λ momentum p_Λ, we employ the following parametrizations suggested in Ref. [62]:

$$\sigma_{\Lambda\rm p\to\Lambda p}(p_\Lambda)=(39.66–100.45x+92.44x^2–21.40x^3)/p_\Lambda\ [\rm mb],\tag{43}$$

$$\sigma_{\Lambda\rm p\to\Sigma^0 p}(p_\Lambda)=(31.10-30.94x+8.16x^2)(p^{\rm cm}_\Sigma/p^{\rm cm}_\Lambda)\ [\rm mb],\tag{44}$$

where $x=$Min(2.1 GeV/c, and p_Λ), $p^{\rm cm}_\Lambda$ and $p^{\rm cm}_\Sigma$ are the corresponding cm momenta. In Eqs. (43) and (44), the momenta are expressed in GeV/c. For the in-medium Λp total cross section we use Eqs. (42)–(44), in which cm momenta $p^{\rm cm}_\Lambda$ and $p^{\rm cm}_\Sigma$ are defined as follows:

$$\begin{aligned}p^{\rm cm}_\Lambda&=\frac{1}{2\sqrt{s_\Lambda}}\lambda[s_\Lambda,m^2_N,(<m^*_\Lambda>)^2],\\p^{\rm cm}_\Sigma&=\frac{1}{2\sqrt{s_\Sigma}}\lambda[s_\Sigma,m^2_N,m^2_{\Sigma^0}],\\s_\Sigma&=s_\Lambda=(E'_\Lambda+m_N)^2-{p'_\Lambda}^2,\end{aligned}\tag{45}$$

where m_{Σ^0} is the Σ^0 hyperon free space mass[1)] and the quantity $\lambda[x,y,z]$ is defined above by Eq. (39).

Let us now modify Eq. (26), describing the respective differential cross section for $\Lambda{\rm K}^+$ production in pA collisions from primary processes (1)–(6), to that corresponding to the kinematical conditions of the ANKE experiment. In this experiment, the differential cross section for production of Λ hyperons in the polar angular range of $0^\circ\leqslant\theta_\Lambda\leqslant6^\circ$ in the lab system in the interaction of protons of energy of 2.83 GeV with the C, Cu, Ag, and Au target nuclei in coincidence with $\rm K^+$ mesons, which were required to have vacuum momenta in the interval of 0.2 GeV/$c\leqslant p_{\rm K^+}\leqslant$ 0.6 GeV/c and to be in the polar angular domain of $0^\circ\leqslant\theta_{\rm K^+}\leqslant12^\circ$, was measured as a function of their vacuum momentum. Performing the respective integration of the full differential cross section

1) Following the predictions of the chiral effective field theory approach [20, 63] and $SU(6)$ quark model [52] for the fate of hyperons in nuclear matter and phenomenological information inferred from hypernuclear data [1, 64] that the Σ hyperon experiences only a moderately repulsive nuclear potential of order 10–40 MeV at central nuclear densities and finite momenta as well as a weakly attractive one at the surface of the nucleus, we assume that the mass of the Σ^0 hyperon is not changed in the nuclear medium.

(26) over the ANKE acceptance window, we can represent this differential cross section in the following form:

$$\left\langle \frac{\mathrm{d}\sigma^{(\mathrm{prim})}_{\mathrm{pA}\to\Lambda\mathrm{X}}(\boldsymbol{p}_0,p_\Lambda)}{\mathrm{d}p_\Lambda \mathrm{d}\boldsymbol{\Omega}_\Lambda} \right\rangle_{\Delta\boldsymbol{\Omega}_\Lambda \Delta\boldsymbol{p}_{\mathrm{K}^+}} = \frac{1}{(2\pi)(1-\cos 6^\circ)} \times \int_{0.2\ \mathrm{GeV}/c}^{0.6\ \mathrm{GeV}/c} \mathrm{d}p_{\mathrm{K}^+} \int_{\cos 12^\circ}^{1} \mathrm{d}\cos\theta_{\mathrm{K}^+} \int_{\cos 6^\circ}^{1} \mathrm{d}\cos\theta_\Lambda \int_0^{2\pi} \mathrm{d}\phi_{\mathrm{K}^+} \int_0^{2\pi} \mathrm{d}\phi_\Lambda \times \frac{\mathrm{d}\sigma^{(\mathrm{prim})}_{\mathrm{pA}\to\Lambda\mathrm{K}^+\mathrm{X}}(\boldsymbol{p}_0,\boldsymbol{p}_\Lambda,\boldsymbol{p}_{\mathrm{K}^+})}{\mathrm{d}\boldsymbol{p}_\Lambda \mathrm{d}\boldsymbol{p}_{\mathrm{K}^+}} p_\Lambda^2 p_{\mathrm{K}^+}^2, \tag{46}$$

where

$$\begin{aligned} &\Delta\boldsymbol{\Omega}_\Lambda = 2\pi(1-\cos 6^\circ), \\ &\Delta\boldsymbol{p}_{\mathrm{K}^+}: 0.2\ \mathrm{GeV}/c \leqslant p_{\mathrm{K}^+} \leqslant 0.6\ \mathrm{GeV}/c, \\ &0^\circ \leqslant \theta_{\mathrm{K}^+} \leqslant 12^\circ. \end{aligned} \tag{47}$$

Here, ϕ_{K^+} and ϕ_Λ are the azimuthal angles of the kaon and Λ hyperon momenta $\boldsymbol{p}_{\mathrm{K}^+}$ and $\boldsymbol{p}_\Lambda$ in the lab system.

2.2 Two-step $\Lambda\mathrm{K}^+$ production mechanisms

At our incident energy of interest, the following two-step processes with pions in an intermediate states contribute mainly (see below) to the $\Lambda\mathrm{K}^+$ production in pA reactions[1)]:

$$\mathrm{p}+\mathrm{N}\to\pi^+,\pi^0,\pi^-+\mathrm{X}; \tag{48}$$

$$\begin{aligned} &\pi^+ + \mathrm{n} \to \Lambda + \mathrm{K}^+, \\ &\pi^0 + \mathrm{p} \to \Lambda + \mathrm{K}^+; \end{aligned} \tag{49}$$

$$\begin{aligned} &\pi^+ + \mathrm{p} \to \Lambda + \pi^+ + \mathrm{K}^+, \\ &\pi^0 + \mathrm{p} \to \Lambda + \pi^0 + \mathrm{K}^+, \\ &\pi^- + \mathrm{p} \to \Lambda + \pi^- + \mathrm{K}^+, \\ &\pi^+ + \mathrm{n} \to \Lambda + \pi^0 + \mathrm{K}^+, \\ &\pi^0 + \mathrm{n} \to \Lambda + \pi^- + \mathrm{K}^+. \end{aligned} \tag{50}$$

Remember that the free threshold energies (or momenta), e.g., for the processes $\pi^+\mathrm{n}\to\Lambda\mathrm{K}^+$ and $\pi^+\mathrm{n}\to\Lambda\pi^0\mathrm{K}^+$, respectively, are 0.76 (0.89) and 1.0 GeV (1.13 GeV/c).

Adopting the results given in Refs. [58, 59], the differential $\Lambda\mathrm{K}^+$ production cross section for pA collisions at small laboratory angles from the secondary channels (49) and (50) can be represented as follows:

$$\frac{\mathrm{d}\sigma^{(\mathrm{sec}),(\pi)}_{\mathrm{pA}\to\Lambda\mathrm{K}^+\mathrm{X}}(\boldsymbol{p}_0,\boldsymbol{p}_\Lambda,\boldsymbol{p}_{\mathrm{K}^+})}{\mathrm{d}\boldsymbol{p}_\Lambda \mathrm{d}\boldsymbol{p}_{\mathrm{K}^+}} = \frac{I_V^{\mathrm{sec}}[A]}{I'_V[A]} \sum_{\pi'=\pi^+,\pi^0,\pi^-} \int_{4\pi} \mathrm{d}\boldsymbol{\Omega}_\pi \int_{p_\pi^{\mathrm{abs}}}^{p_\pi^{\mathrm{lim}}(\vartheta_\pi)} p_\pi^2 \mathrm{d}p_\pi \frac{\mathrm{d}\sigma^{(\mathrm{prim})}_{\mathrm{pA}\to\pi'\mathrm{X}}(\boldsymbol{p}_0)}{\mathrm{d}\boldsymbol{p}_\pi} \times \left[\frac{Z}{A} \left\langle \frac{\mathrm{d}\sigma_{\pi'\mathrm{p}\to\Lambda\mathrm{K}^+\mathrm{X}}(\boldsymbol{p}_\pi,\boldsymbol{p}'_\Lambda,\boldsymbol{p}'_{\mathrm{K}^+})}{\mathrm{d}\boldsymbol{p}'_\Lambda \mathrm{d}\boldsymbol{p}'_{\mathrm{K}^+}} \right\rangle_A + \frac{N}{A} \left\langle \frac{\mathrm{d}\sigma_{\pi'\mathrm{n}\to\Lambda\mathrm{K}^+\mathrm{X}}(\boldsymbol{p}_\pi,\boldsymbol{p}'_\Lambda,\boldsymbol{p}'_{\mathrm{K}^+})}{\mathrm{d}\boldsymbol{p}'_\Lambda \mathrm{d}\boldsymbol{p}'_{\mathrm{K}^+}} \right\rangle_A \right] \frac{\mathrm{d}\boldsymbol{p}'_\Lambda}{\mathrm{d}\boldsymbol{p}_\Lambda} \frac{\mathrm{d}\boldsymbol{p}'_{\mathrm{K}^+}}{\mathrm{d}\boldsymbol{p}_{\mathrm{K}^+}}, \tag{51}$$

where

$$\begin{aligned} I_V^{\mathrm{sec}}[A] = {} & 2\pi A^2 \int_0^R r_\perp \mathrm{d}r_\perp \int_{-\sqrt{R^2-r_\perp^2}}^{\sqrt{R^2-r_\perp^2}} \mathrm{d}z \rho(\sqrt{r_\perp^2+z^2}) \int_0^{\sqrt{R^2-r_\perp^2}-z} \mathrm{d}l \rho(\sqrt{r_\perp^2+(z+l)^2}) \\ & \times \exp\left[-\sigma^{\mathrm{in}}_{\mathrm{pN}} A \int_{-\sqrt{R^2-r_\perp^2}}^{z} \rho(\sqrt{r_\perp^2+x^2}) \mathrm{d}x - \sigma^{\mathrm{tot}}_{\pi' N} A \int_z^{z+l} \rho(\sqrt{r_\perp^2+x^2}) \mathrm{d}x \right] \\ & \times \exp\left[-\sigma^{\mathrm{tot}}_{\mathrm{K}^+\mathrm{N}} A \int_{z+l}^{\sqrt{R^2-r_\perp^2}} \rho(\sqrt{r_\perp^2+x^2}) \mathrm{d}x - \sigma^{\mathrm{tot}}_{\Lambda N}(p'_\Lambda) A \int_{z+l}^{\sqrt{R^2-r_\perp^2}} \rho(\sqrt{r_\perp^2+x^2}) \mathrm{d}x \right], \end{aligned} \tag{52}$$

and

$$\left\langle \frac{\mathrm{d}\sigma_{\pi'\mathrm{N}\to\Lambda\mathrm{K}^+\mathrm{X}}(\boldsymbol{p}_\pi,\boldsymbol{p}'_\Lambda,\boldsymbol{p}'_{\mathrm{K}^+})}{\mathrm{d}\boldsymbol{p}'_\Lambda \mathrm{d}\boldsymbol{p}'_{\mathrm{K}^+}} \right\rangle_A = \int\int P_A(\boldsymbol{p}_t,E) \mathrm{d}\boldsymbol{p}_t \mathrm{d}E \left\{ \frac{\mathrm{d}\sigma_{\pi'\mathrm{N}\to\Lambda\mathrm{K}^+\mathrm{X}}[\sqrt{s_1}, <m^*_{\mathrm{K}^+}>, <m^*_\Lambda>, \boldsymbol{p}'_\Lambda, \boldsymbol{p}'_{\mathrm{K}^+}]}{\mathrm{d}\boldsymbol{p}'_\Lambda \mathrm{d}\boldsymbol{p}'_{\mathrm{K}^+}} \right\}. \tag{53}$$

1) We assume that the Δ resonance, produced by first-chance pN collisions, decays into π and nucleon immediately after its production in these collisions. This assumption is well justified due to the following. The Δ decay mean free path can be evaluated as $\lambda^{\mathrm{dec}}_\Delta = p_\Delta/(m_\Delta \Gamma_\Delta)$, where p_Δ, m_Δ and Γ_Δ are the Δ resonance laboratory momentum, pole mass and width, respectively. For typical values $p_\Delta \approx m_\Delta$ and $\Gamma_\Delta \approx 120$ MeV, we obtain that $\lambda^{\mathrm{dec}}_\Delta \approx 1.7$ fm. The Δ mean free path up to inelastic interaction can be estimated as $\lambda^{\mathrm{in}}_\Delta = 1/(<\rho_N>\sigma^{\mathrm{in}}_{\Delta N})$, where $\sigma^{\mathrm{in}}_{\Delta N}$ is the appropriate ΔN inelastic cross section. Using $<\rho_N> = 0.55\rho_0$ (^{12}C target nucleus), $\rho_0 = 0.16$ fm^{-3}, and as an estimate of $\sigma^{\mathrm{in}}_{\Delta N}$ the relation $\sigma^{\mathrm{in}}_{\Delta N} = \frac{3}{4}\sigma^{\mathrm{in}}_{\mathrm{pN}}$ (cf. second Ref. from Ref. [11]) with value $\sigma^{\mathrm{in}}_{\mathrm{pN}} = 30$ mb, we get that $\lambda^{\mathrm{in}}_\Delta \approx 5.1$ fm. The latter value is three times larger than the estimated above Δ decay mean free path.

Here, $\mathrm{d}\sigma^{(\mathrm{prim})}_{\mathrm{pA}\to\pi'\mathrm{X}}(\boldsymbol{p}_0)/\mathrm{d}\boldsymbol{p}_\pi$ are the inclusive differential cross sections for pion production on nuclei at small laboratory angles and for high momenta from the primary proton-induced reaction channel (48); $\mathrm{d}\sigma_{\pi'\mathrm{N}\to\Lambda\mathrm{K}^+\mathrm{X}}[\sqrt{s_1},<m^*_{\mathrm{K}^+}>,<m^*_\Lambda>,\boldsymbol{p}'_\Lambda,\boldsymbol{p}'_{\mathrm{K}^+}]/\mathrm{d}\boldsymbol{p}'_\Lambda\mathrm{d}\boldsymbol{p}'_{\mathrm{K}^+}$ are the "in-medium" differential cross sections for Λ and K^+ creation with effective masses $<m^*_\Lambda>$ and $<m^*_{\mathrm{K}^+}>$ and with the in-medium momenta $\boldsymbol{p}'_\Lambda$ and $\boldsymbol{p}'_{\mathrm{K}^+}$, respectively, in reactions (49) and (50) at the $\pi' N$ center-of-mass energy $\sqrt{s_1}$. This and the other quantities in Eq. (51) and (52) are defined in Refs. [44, 57] as well as by Eqs. (29) and (42)–(45). For the cross sections $d\sigma^{(\mathrm{prim})}_{\mathrm{pA}\to\pi'\mathrm{X}}(\boldsymbol{p}_0)/d\boldsymbol{p}_\pi$, we use the respective parametrizations of the experimental pion yields at small angles and for high momenta [44] in our calculations of the $\Lambda\mathrm{K}^+$ cross sections from the two-step processes (48)–(50). For ^{63}Cu target nucleus they were taken from Ref. [44]. For $\Lambda\mathrm{K}^+$ production calculations in the cases of ^{12}C and ^{108}Ag, ^{197}Au target nuclei presented below, we have supposed that the ratio of the differential cross section for pion creation on ^{12}C and on these nuclei from the primary process (48) to the effective number of target nucleons participating in it (quantity $I'_V[A]$ in Eq. (51)) is the same as that for ^{9}Be and ^{63}Cu adjusted for kinematics, relating, respectively, to ^{12}C and ^{108}Ag, ^{197}Au. For the ^{9}Be target nucleus the parametrizations of the experimental pion differential cross sections at small angles and for high momenta were borrowed from Ref. [44]. Within the representation of Eqs. (49) and (50), the cross sections $\mathrm{d}\sigma_{\pi'\mathrm{N}\to\Lambda\mathrm{K}^+\mathrm{X}}[\sqrt{s_1},<m^*_{\mathrm{K}^+}>,<m^*_\Lambda>,\boldsymbol{p}'_\Lambda,\boldsymbol{p}'_{\mathrm{K}^+}]/\mathrm{d}\boldsymbol{p}'_\Lambda\mathrm{d}\boldsymbol{p}'_{\mathrm{K}^+}$ can be written in the following forms:

$$\frac{\mathrm{d}\sigma_{\pi^+\mathrm{p}\to\Lambda\mathrm{K}^+\mathrm{X}}[\sqrt{s_1},<m^*_{\mathrm{K}^+}>,<m^*_\Lambda>,\boldsymbol{p}'_\Lambda,\boldsymbol{p}'_{\mathrm{K}^+}]}{\mathrm{d}\boldsymbol{p}'_\Lambda\mathrm{d}\boldsymbol{p}'_{\mathrm{K}^+}} = \frac{\mathrm{d}\sigma_{\pi^+\mathrm{p}\to\Lambda\pi^+\mathrm{K}^+}[\sqrt{s_1},<m^*_{\mathrm{K}^+}>,<m^*_\Lambda>,\boldsymbol{p}'_\Lambda,\boldsymbol{p}'_{\mathrm{K}^+}]}{\mathrm{d}\boldsymbol{p}'_\Lambda\mathrm{d}\boldsymbol{p}'_{\mathrm{K}^+}}, \quad (54)$$

$$\frac{\mathrm{d}\sigma_{\pi^0\mathrm{p}\to\Lambda\mathrm{K}^+\mathrm{X}}[\sqrt{s_1},<m^*_{\mathrm{K}^+}>,<m^*_\Lambda>,\boldsymbol{p}'_\Lambda,\boldsymbol{p}'_{\mathrm{K}^+}]}{\mathrm{d}\boldsymbol{p}'_\Lambda\mathrm{d}\boldsymbol{p}'_{\mathrm{K}^+}} = \frac{\mathrm{d}\sigma_{\pi^0\mathrm{p}\to\Lambda\mathrm{K}^+}[\sqrt{s_1},<m^*_{\mathrm{K}^+}>,<m^*_\Lambda>,\boldsymbol{p}'_\Lambda,\boldsymbol{p}'_{\mathrm{K}^+}]}{\mathrm{d}\boldsymbol{p}'_\Lambda\mathrm{d}\boldsymbol{p}'_{\mathrm{K}^+}} + \frac{\mathrm{d}\sigma_{\pi^0\mathrm{p}\to\Lambda\pi^0\mathrm{K}^+}[\sqrt{s_1},<m^*_{\mathrm{K}^+}>,<m^*_\Lambda>,\boldsymbol{p}'_\Lambda,\boldsymbol{p}'_{\mathrm{K}^+}]}{\mathrm{d}\boldsymbol{p}'_\Lambda\mathrm{d}\boldsymbol{p}'_{\mathrm{K}^+}}, \quad (55)$$

$$\frac{\mathrm{d}\sigma_{\pi^-\mathrm{p}\to\Lambda\mathrm{K}^+\mathrm{X}}[\sqrt{s_1},<m^*_{\mathrm{K}^+}>,<m^*_\Lambda>,\boldsymbol{p}'_\Lambda,\boldsymbol{p}'_{\mathrm{K}^+}]}{\mathrm{d}\boldsymbol{p}'_\Lambda\mathrm{d}\boldsymbol{p}'_{\mathrm{K}^+}} = \frac{\mathrm{d}\sigma_{\pi^-\mathrm{p}\to\Lambda\pi^-\mathrm{K}^+}[\sqrt{s_1},<m^*_{\mathrm{K}^+}>,<m^*_\Lambda>,\boldsymbol{p}'_\Lambda,\boldsymbol{p}'_{\mathrm{K}^+}]}{\mathrm{d}\boldsymbol{p}'_\Lambda\mathrm{d}\boldsymbol{p}'_{\mathrm{K}^+}}, \quad (56)$$

$$\frac{\mathrm{d}\sigma_{\pi^+\mathrm{n}\to\Lambda\mathrm{K}^+\mathrm{X}}[\sqrt{s_1},<m^*_{\mathrm{K}^+}>,<m^*_\Lambda>,\boldsymbol{p}'_\Lambda,\boldsymbol{p}'_{\mathrm{K}^+}]}{\mathrm{d}\boldsymbol{p}'_\Lambda\mathrm{d}\boldsymbol{p}'_{\mathrm{K}^+}} = \frac{\mathrm{d}\sigma_{\pi^+\mathrm{n}\to\Lambda\mathrm{K}^+}[\sqrt{s_1},<m^*_{\mathrm{K}^+}>,<m^*_\Lambda>,\boldsymbol{p}'_\Lambda,\boldsymbol{p}'_{\mathrm{K}^+}]}{\mathrm{d}\boldsymbol{p}'_\Lambda\mathrm{d}\boldsymbol{p}'_{\mathrm{K}^+}} + \frac{\mathrm{d}\sigma_{\pi^+\mathrm{n}\to\Lambda\pi^0\mathrm{K}^+}[\sqrt{s_1},<m^*_{\mathrm{K}^+}>,<m^*_\Lambda>,\boldsymbol{p}'_\Lambda,\boldsymbol{p}'_{\mathrm{K}^+}]}{\mathrm{d}\boldsymbol{p}'_\Lambda\mathrm{d}\boldsymbol{p}'_{\mathrm{K}^+}}, \quad (57)$$

$$\frac{\mathrm{d}\sigma_{\pi^0\mathrm{n}\to\Lambda\mathrm{K}^+\mathrm{X}}[\sqrt{s_1},<m^*_{\mathrm{K}^+}>,<m^*_\Lambda>,\boldsymbol{p}'_\Lambda,\boldsymbol{p}'_{\mathrm{K}^+}]}{\mathrm{d}\boldsymbol{p}'_\Lambda\mathrm{d}\boldsymbol{p}'_{\mathrm{K}^+}} = \frac{\mathrm{d}\sigma_{\pi^0\mathrm{n}\to\Lambda\pi^-\mathrm{K}^+}[\sqrt{s_1},<m^*_{\mathrm{K}^+}>,<m^*_\Lambda>,\boldsymbol{p}'_\Lambda,\boldsymbol{p}'_{\mathrm{K}^+}]}{\mathrm{d}\boldsymbol{p}'_\Lambda\mathrm{d}\boldsymbol{p}'_{\mathrm{K}^+}}, \quad (58)$$

$$\frac{\mathrm{d}\sigma_{\pi^-\mathrm{n}\to\Lambda\mathrm{K}^+\mathrm{X}}[\sqrt{s_1},<m^*_{\mathrm{K}^+}>,<m^*_\Lambda>,\boldsymbol{p}'_\Lambda,\boldsymbol{p}'_{\mathrm{K}^+}]}{\mathrm{d}\boldsymbol{p}'_\Lambda\mathrm{d}\boldsymbol{p}'_{\mathrm{K}^+}} = 0, \quad (59)$$

where $\mathrm{d}\sigma_{\pi'\mathrm{N}\to\Lambda\mathrm{K}^+}[\sqrt{s_1},<m^*_{\mathrm{K}^+}>,<m^*_\Lambda>,\boldsymbol{p}'_\Lambda,\boldsymbol{p}'_{\mathrm{K}^+}]/\mathrm{d}\boldsymbol{p}'_\Lambda\mathrm{d}\boldsymbol{p}'_{\mathrm{K}^+}$ and $\mathrm{d}\sigma_{\pi'\mathrm{N}\to\Lambda\pi\mathrm{K}^+}[\sqrt{s_1},<m^*_{\mathrm{K}^+}>,<m^*_\Lambda>,\boldsymbol{p}'_\Lambda,\boldsymbol{p}'_{\mathrm{K}^+}]/\mathrm{d}\boldsymbol{p}'_\Lambda\mathrm{d}\boldsymbol{p}'_{\mathrm{K}^+}$ are the "in-medium" differential cross sections of reaction channels (49) and (50), correspondingly. Taking into account the two-body kinematics of elementary processes (49) as well as the isospin symmetry, we get the following expressions for the former ones:

$$\begin{aligned}\frac{\mathrm{d}\sigma_{\pi^+\mathrm{n}\to\Lambda\mathrm{K}^+}[\sqrt{s_1},<m^*_{\mathrm{K}^+}>,<m^*_\Lambda>,\boldsymbol{p}'_\Lambda,\boldsymbol{p}'_{\mathrm{K}^+}]}{\mathrm{d}\boldsymbol{p}'_\Lambda\mathrm{d}\boldsymbol{p}'_{\mathrm{K}^+}} &= \frac{\pi}{I_2(s_1,<m^*_{\mathrm{K}^+}>,<m^*_\Lambda>)E'_\Lambda}\\ &\times\frac{\mathrm{d}\sigma_{\pi^+\mathrm{n}\to\Lambda\mathrm{K}^+}(\sqrt{s_1},<m^*_{\mathrm{K}^+}>,<m^*_\Lambda>,\theta^*_\Lambda)}{\mathrm{d}\boldsymbol{\Omega}^*_\Lambda}\\ &\times\frac{1}{(\omega_0+E_t)}\delta\left[\omega_0+E_t-\sqrt{(<m^*_{\mathrm{K}^+}>)^2+\boldsymbol{p}'^2_{\mathrm{K}^+}}\right]\\ &\times\delta(\boldsymbol{Q}_0+\boldsymbol{p}_t-\boldsymbol{p}'_{\mathrm{K}^+}),\end{aligned} \quad (60)$$

$$\frac{\mathrm{d}\sigma_{\pi^0\mathrm{p}\to\Lambda\mathrm{K}^+}[\sqrt{s_1},<m^*_{\mathrm{K}^+}>,<m^*_\Lambda>,\boldsymbol{p}'_\Lambda,\boldsymbol{p}'_{\mathrm{K}^+}]}{\mathrm{d}\boldsymbol{p}'_\Lambda\mathrm{d}\boldsymbol{p}'_{\mathrm{K}^+}} = \frac{1}{2}\frac{\mathrm{d}\sigma_{\pi^+\mathrm{n}\to\Lambda\mathrm{K}^+}[\sqrt{s_1},<m^*_{\mathrm{K}^+}>,<m^*_\Lambda>,\boldsymbol{p}'_\Lambda,\boldsymbol{p}'_{\mathrm{K}^+}]}{\mathrm{d}\boldsymbol{p}'_\Lambda\mathrm{d}\boldsymbol{p}'_{\mathrm{K}^+}}. \quad (61)$$

Here,

$$\omega_0 = E_\pi - E'_\Lambda, \boldsymbol{Q}_0 = \boldsymbol{p}_\pi - \boldsymbol{p}'_\Lambda, \quad (62)$$

where $\boldsymbol{p}_\pi$ and E_π are the momentum and total energy respectively of an intermediate pion (which is assumed to be on-shell), and I_2 is the two-body phase space, defined as [58]:

$$I_2(s_1,<m^*_{\mathrm{K}^+}>,<m^*_\Lambda>) = \left(\frac{\pi}{2}\right)\frac{\lambda[s_1,(<m^*_{\mathrm{K}^+}>)^2,(<m^*_\Lambda>)^2]}{s_1}. \quad (63)$$

In Eq. (60), $\mathrm{d}\sigma_{\pi^+\mathrm{n}\to\Lambda\mathrm{K}^+}(\sqrt{s_1},<m^*_{\mathrm{K}^+}>,<m^*_\Lambda>,\theta^*_\Lambda)/\mathrm{d}\boldsymbol{\Omega}^*_\Lambda$ is the Λ "in-medium" differential cross section in the $\pi^+ n$ center-of-mass system. As earlier, we assume that this cross section is equivalent to the vacuum cross section $\mathrm{d}\sigma_{\pi^+\mathrm{n}\to\Lambda\mathrm{K}^+}(\sqrt{s_1},m_{\mathrm{K}^+},m_\Lambda,\theta^*_\Lambda)/\mathrm{d}\boldsymbol{\Omega}^*_\Lambda$ in which the

free kaon and Λ hyperon masses $m_{\rm K^+}$ and m_Λ are replaced by the in-medium masses $<m^*_{\rm K^+}>$ and $<m^*_\Lambda>$. As in Refs. [60, 65], we choose the free Λ angular distribution in the following form:

$$\frac{{\rm d}\sigma_{\pi^+{\rm n}\to\Lambda{\rm K}^+}(\sqrt{s_1},m_{\rm K^+},m_\Lambda,\theta^*_\Lambda)}{{\rm d}\boldsymbol{\Omega}^*_\Lambda} = [1-A_1(\sqrt{s_1},\sqrt{\tilde{s}_{\rm th}})\cos\theta^*_\Lambda]\frac{\sigma_{\pi^+{\rm n}\to\Lambda{\rm K}^+}(\sqrt{s_1},\sqrt{\tilde{s}_{\rm th}})}{4\pi}, \quad (64)$$

$$A_1(\sqrt{s_1},\sqrt{\tilde{s}_{\rm th}})=\begin{cases} 5.26\left(\dfrac{\sqrt{s_1}-\sqrt{\tilde{s}_{\rm th}}}{\rm GeV}\right) & \text{for } \sqrt{\tilde{s}_{\rm th}}<\sqrt{s_1}\leqslant 1.8 \text{ GeV}, \\ 1 & \text{for } \sqrt{s_1}>1.8 \text{ GeV}, \end{cases} \quad (65)$$

$$\sigma_{\pi^+{\rm n}\to\Lambda{\rm K}^+}(\sqrt{s_1},\sqrt{\tilde{s}_{\rm th}})=\begin{cases} 10.0\left(\dfrac{\sqrt{s_1}-\sqrt{\tilde{s}_{\rm th}}}{\rm GeV}\right) \text{ [mb]} & \text{for } \sqrt{\tilde{s}_{\rm th}}<\sqrt{s_1}\leqslant 1.7 \text{ GeV}, \\ 0.09\left(\dfrac{\rm GeV}{\sqrt{s_1}-1.6 \text{ GeV}}\right) \text{ [mb]} & \text{for } \sqrt{s_1}>1.7 \text{ GeV}, \end{cases} \quad (66)$$

where $\sqrt{\tilde{s}_{\rm th}} = m_\Lambda + m_{\rm K^+}$ is the free threshold energy. In our calculations of the $\Lambda{\rm K}^+$ pair production on nuclei, the "in-medium" differential cross sections ${\rm d}\sigma_{\pi'{\rm N}\to\Lambda\pi{\rm K}^+}[\sqrt{s_1},<m^*_{\rm K^+}>,<m^*_\Lambda>,\boldsymbol{p}'_\Lambda,\boldsymbol{p}'_{\rm K^+}]/{\rm d}\boldsymbol{p}'_\Lambda{\rm d}\boldsymbol{p}'_{\rm K^+}$ of reaction channels (50) have been described according to the three-body phase space. Following Eq. (36), one has:

$$\begin{aligned}&\frac{{\rm d}\sigma_{\pi'{\rm N}\to\Lambda\pi{\rm K}^+}[\sqrt{s_1},<m^*_{\rm K^+}>,<m^*_\Lambda>,\boldsymbol{p}'_\Lambda,\boldsymbol{p}'_{\rm K^+}]}{{\rm d}\boldsymbol{p}'_\Lambda{\rm d}\boldsymbol{p}'_{\rm K^+}} \\ =\ &\frac{1}{8E'_\Lambda E'_{\rm K^+}}\times\frac{\sigma_{\pi' N\to\Lambda\pi K^+}(\sqrt{s_1},\sqrt{\tilde{s}^*_{\rm 1th}})}{I_3(s_1,<m^*_{\rm K^+}>,m_\pi,<m^*_\Lambda>)}\frac{1}{(\omega_1+E_t)} \\ &\times\delta\left(\omega_1+E_t-\sqrt{m^2_\pi+(\boldsymbol{Q}_1+\boldsymbol{p}_t)^2}\right), \end{aligned} \quad (67)$$

where

$$\omega_1=E_\pi-E'_\Lambda-E'_{\rm K^+},\ \boldsymbol{Q}_1=\boldsymbol{p}_\pi-\boldsymbol{p}'_\Lambda-\boldsymbol{p}'_{\rm K^+} \quad (68)$$

and $\sqrt{\tilde{s}^*_{\rm 1th}}=<m^*_\Lambda>+m_\pi+<m^*_{\rm K^+}>$ is the in-medium threshold energy. In Eq. (67), $\sigma_{\pi'{\rm N}\to\Lambda\pi{\rm K}^+}(\sqrt{s_1},\sqrt{\tilde{s}^*_{\rm 1th}})$ are the "in-medium" total cross sections for $\Lambda{\rm K}^+$ pair production in the reactions (50). As before, we assume that these cross sections are equivalent to the vacuum cross sections $\sigma_{\pi'{\rm N}\to\Lambda\pi{\rm K}^+}(\sqrt{s_1},\sqrt{\tilde{s}_{\rm 1th}})$ in which the free threshold energy $\sqrt{\tilde{s}_{\rm 1th}}=m_\Lambda+m_\pi+m_{\rm K^+}$ is replaced by the in-medium threshold $\sqrt{\tilde{s}^*_{\rm 1th}}$. In line with Ref. [35], for the free total cross sections $\sigma_{\pi'{\rm N}\to\Lambda\pi{\rm K}^+}(\sqrt{s_1},\sqrt{\tilde{s}_{\rm 1th}})$ we have adopted the following expression:

$$\begin{aligned}&\sigma_{\pi^+{\rm p}\to\Lambda\pi^+{\rm K}^+}(\sqrt{s_1},\sqrt{\tilde{s}_{\rm 1th}}) \\ \approx\ &\sigma_{\pi^0{\rm p}\to\Lambda\pi^0{\rm K}^+}(\sqrt{s_1},\sqrt{\tilde{s}_{\rm 1th}})\approx\sigma_{\pi^-{\rm p}\to\Lambda\pi^-{\rm K}^+}(\sqrt{s_1},\sqrt{\tilde{s}_{\rm 1th}}) \\ \approx\ &\sigma_{\pi^+{\rm n}\to\Lambda\pi^0{\rm K}^+}(\sqrt{s_1},\sqrt{\tilde{s}_{\rm 1th}})\approx\sigma_{\pi^0{\rm n}\to\Lambda\pi^-{\rm K}^+}(\sqrt{s_1},\sqrt{\tilde{s}_{\rm 1th}}) \\ \approx\ &24.0\left(1-\frac{\tilde{s}_{\rm 1th}}{s_1}\right)^{3.16}\left(\frac{\tilde{s}_{\rm 1th}}{s_1}\right)^{4.24} \text{ [mb]}. \end{aligned} \quad (69)$$

It is worth mentioning that, as follows from Eqs. (66), (69) and Ref. [66], the $\Lambda{\rm K}^+$ production cross sections in the secondary pion–nucleon processes (49) and (50) are substantially larger than those in the four-body reaction channels $\pi'{\rm N}\to\Lambda\pi\pi{\rm K}^+$ at pion momenta $\leqslant$ 2 GeV/c, giving, as our estimate shows, the main contribution to the $\Lambda{\rm K}^+$ creation on nuclei for kinematics of interest. Therefore, we discard the latter in the present study.

In addition to the two-step processes with intermediate pions (48)–(50) we consider the following production/decay sequence, which may contribute to the $\Lambda{\rm K}^+$ yield from nuclei in the conditions of the ANKE experiment at the incident proton beam energy of interest:

$${\rm p+p}\to\Sigma^0+{\rm p}+{\rm K}^+, \quad (70)$$

$${\rm p+n}\to\Sigma^0+{\rm n}+{\rm K}^+, \quad (71)$$

$$\Sigma^0\to\Lambda+\gamma. \quad (72)$$

Presently, there are four sets of data available for the total cross section $\sigma_{{\rm pp}\to\Sigma^0{\rm pK}^+}$ of reaction (70). Three of these have recently been taken by the COSY-11 [24, 25], COSY-TOF [28] and ANKE [29] Collaborations at proton energies $\leqslant$ 2.4 GeV, whereas the other was obtained a long time ago at beam energies $\geqslant$ 2.85 GeV [21]. The comparison of these data with the results of calculations by parametrization

$$\sigma_{{\rm pp}\to\Sigma^0{\rm pK}^+}(\sqrt{s},\sqrt{s_0})=\begin{cases} \dfrac{A_{\Sigma^0}(s-s_0)^2}{4m^2_{\rm p}+B_{\Sigma^0}(s-s_0)^2} & \text{for } 0.225 \text{ GeV}<\sqrt{s}-\sqrt{s_0}<2.0 \text{ GeV}, \\ C_{\Sigma^0}\left(\sqrt{s}-\sqrt{s_0}\right)^2 & \text{for } 0<\sqrt{s}-\sqrt{s_0}\leqslant 0.225 \text{ GeV}, \end{cases} \quad (73)$$

(solid line) is shown in Fig. 4. In Eq. (73), $\sqrt{s_0} = m_{\Sigma^0}+m_{\rm p}+m_{\rm K^+}$ is the threshold energy and the constants A_{Σ^0}, B_{Σ^0} and C_{Σ^0} are given as 26.0 μb/GeV^2, 1/GeV^2 and 154.5 μb/GeV^2, respectively. The "low" excess energy part of Eq. (73) was taken from Ref. [28]. The parametrization (73) fits well the full available set of data for the pp→Σ^0pK$^+$ process[1)].

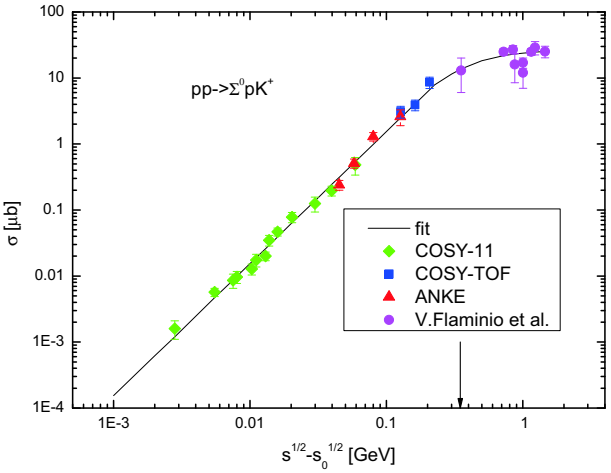

Fig. 4. (color online) Total cross section for the pp → Σ^0pK$^+$ reaction as a function of excess energy. The arrow indicates the excess energy, which corresponds to the proton kinetic energy of 2.83 GeV. For further notation see the text.

Direct data on the total cross section $\sigma_{\rm pn\to\Sigma^0nK^+}$ of reaction (71) do not currently exist. Reference [21] only has three data points for the total cross section $\sigma_{\rm pn\to\Sigma^0pK^0}$ of the channel pn→Σ^0pK^0 at 5.135, 6.124 and 16.088 GeV initial energies, which due to the isospin symmetry is equal to the former one. Comparing these with the data that are available [21] for the pp→Σ^0pK$^+$ process at similar energies (at energies of 5.135 and 6.045 GeV), one can readily find that at these energies the ratio of the pn and pp total cross sections $\sigma_{\rm pn\to\Sigma^0pK^0}/\sigma_{\rm pp\to\Sigma^0pK^+}$ varies approximately from 0.5 to 1.5. Therefore, it is natural to take for this ratio here an average value of one, which means that:

$$\sigma_{\rm pn\to\Sigma^0pK^0}(\sqrt{s})=\sigma_{\rm pn\to\Sigma^0nK^+}(\sqrt{s})\approx\sigma_{\rm pp\to\Sigma^0pK^+}(\sqrt{s},\sqrt{s_0}) \tag{74}$$

at the high incident proton kinetic energies considered. Due to the lack of data at lower beam energies, we will also adopt Eq. (74) at all collision energies $\sqrt{s}$, accessible in the calculation of ΛK$^+$ production in pA interactions from the production/decay sequence (70)–(72) at the initial energy of 2.83 GeV. At this energy the ratio $R_{\Sigma^0/\Lambda}$ of the total cross sections $\sigma_{\rm pp\to\Sigma^0pK^+}$ and $\sigma_{\rm pp\to\Lambda pK^+}$, shown in Figs. 4 and 1, is about 1/4. Hence, the production/decay chain (70)–(72) may indeed contribute to the (p,ΛK$^+$) reaction on nuclei for our initial energy of interest. The total cross section of the subprocess pp→Σ^0pπ^0K$^+$ with additional pion in the final state, assuming that it goes completely through the reaction pp→Λ(1405)pK$^+$, is (1.5±0.7) μb at beam energy of 2.83 GeV [67]. This cross section is substantially lower than that for the pp→Σ^0pK$^+$ process, shown in Fig. 4, at this energy. Therefore, we will neglect the contribution from the production/decay chain pN→Σ^0Nπ^0K$^+$, $\Sigma^0\to\Lambda\gamma$ in our calculations of the ΛK$^+$ yield in pA collisions at 2.83 GeV incident energy.

The Σ^0 hyperons and K$^+$ mesons produced in elementary processes (70), (71) are mainly emitted in the forward direction. Most of the Σ^0's decay into Λ and γ essentially outside the target nuclei of interest. Taking into account these facts and neglecting the change of the Σ^0 mass in the nuclear medium but accounting for the in-medium modifications of the masses of other final hadrons (kaons and nucleons) participating in these processes on the same footing as that employed in calculating the ΛK$^+$ production cross section (26) from the primary proton-induced reaction channels (1)–(6), as well as using the results given in Refs. [68, 69], we get the following expression for the ΛK$^+$ creation cross section for pA interactions from this chain:

$$\frac{{\rm d}\sigma^{({\rm sec}),(\Sigma^0)}_{\rm pA\to\Lambda K^+X}(\boldsymbol{p}_0,\boldsymbol{p}_\Lambda,\boldsymbol{p}_{\rm K^+})}{{\rm d}\boldsymbol{p}_\Lambda{\rm d}\boldsymbol{p}_{\rm K^+}} = I_{\rm K^+\Sigma^0}[A]\int{\rm d}\boldsymbol{p}_{\Sigma^0}\left[\frac{Z}{A}\left\langle\frac{{\rm d}\sigma_{\rm pp\to\Sigma^0pK^+}(\boldsymbol{p}'_0,\boldsymbol{p}_{\Sigma^0},\boldsymbol{p}'_{\rm K^+})}{{\rm d}\boldsymbol{p}_{\Sigma^0}{\rm d}\boldsymbol{p}'_{\rm K^+}}\right\rangle_A+\frac{N}{A}\left\langle\frac{{\rm d}\sigma_{\rm pn\to\Sigma^0nK^+}(\boldsymbol{p}'_0,\boldsymbol{p}_{\Sigma^0},\boldsymbol{p}'_{\rm K^+})}{{\rm d}\boldsymbol{p}_{\Sigma^0}{\rm d}\boldsymbol{p}'_{\rm K^+}}\right\rangle_A\right]$$
$$\times\frac{{\rm d}\boldsymbol{p}'_{\rm K^+}}{{\rm d}\boldsymbol{p}_{\rm K^+}}\frac{BR(\Sigma^0\to\Lambda\gamma)\theta(E_{\Sigma^0}-E_\Lambda)}{4I_2(m^2_{\Sigma^0},m^2_\Lambda,0)E_\Lambda(E_{\Sigma^0}-E_\Lambda)}\delta\left(E_{\Sigma^0}-E_\Lambda-\sqrt{(\boldsymbol{p}_{\Sigma^0}-\boldsymbol{p}_\Lambda)^2}\right), \tag{75}$$

where $\boldsymbol{p}_{\Sigma^0}$ and E_{Σ^0} are the vacuum momentum and total energy of a Σ^0 hyperon ($E_{\Sigma^0}=\sqrt{m^2_{\Sigma^0}+\boldsymbol{p}^2_{\Sigma^0}}$), $\theta(x)$ is the standard step function and $BR(\Sigma^0\to\Lambda\gamma)=1$. The averaged differential cross sections $\langle{\rm d}\sigma_{\rm pN\to\Sigma^0NK^+}(\boldsymbol{p}'_0,\boldsymbol{p}_{\Sigma^0},\boldsymbol{p}'_{\rm K^+})/{\rm d}\boldsymbol{p}_{\Sigma^0}{\rm d}\boldsymbol{p}'_{\rm K^+}\rangle_A$, in Eq. (75), are defined by Eqs. (28), (36) and (37), in which one has to make the following substitutions: $\boldsymbol{p}'_\Lambda\to\boldsymbol{p}_{\Sigma^0}$, $E'_\Lambda\to E_{\Sigma^0}$, $<m^*_\Lambda>\to m_{\Sigma^0}$ and $\sigma_{\rm pN\to\Lambda K^+X}(\sqrt{s},\sqrt{s^*_{\rm th}},\sqrt{s^*_{\rm 1th}},\sqrt{s^*_{\rm 2th}})\to$

1) This parametrization is also consistent with the cross section of (16.5±20%) μb for channel pp→Σ^0pK$^+$ at beam energy of 3.5 GeV ($\sqrt{s}-\sqrt{s_0}$=0.555 GeV) evaluated in Ref. [30], by dividing the measured cross section for the pp→ΛpK$^+$ reaction at this energy by a factor of 2.2, and assuming an uncertainty of 20%.

$\sigma_{\rm pN\to\Sigma^0NK^+}(\sqrt{s},\sqrt{s_0^*})$, where $\sqrt{s_0^*}=m_{\Sigma^0}+<m_{\rm p}^*>+<m_{\rm K^+}^*>$. The quantity $I_{\rm K^+\Sigma^0}[A]$ in Eq. (75) is defined above by Eq. (27), in which one has to replace $\sigma_{\Lambda N}^{\rm tot}$ by inelastic cross section $\sigma_{\Sigma^0 N}^{\rm in}$ of the Σ^0N interaction[1)]. Due to isospin symmetry, this cross section is the same as the inelastic cross sections $\sigma_{\Sigma^0 p}^{\rm in}$ and $\sigma_{\Sigma^0 n}^{\rm in}$ of the Σ^0p and $\Sigma^0 n$ interactions. At Σ^0 momenta of interest, the cross section $\sigma_{\Sigma^0 p}^{\rm in}$ is exhausted by the total cross sections $\sigma_{\Sigma^0 p\to\Lambda p}$ and $\sigma_{\Sigma^0 p\to\Sigma^+ n}$ of the inelastic $\Sigma^0 p\to\Lambda p$ and $\Sigma^0 p\to\Sigma^+ n$ processes:

$$\sigma_{\Sigma^0 N}^{\rm in}=\sigma_{\Sigma^0 p}^{\rm in}=\sigma_{\Sigma^0 p\to\Lambda p}+\sigma_{\Sigma^0 p\to\Sigma^+ n}. \tag{76}$$

The first cross section in Eq. (76) is obtained by detailed balance [62]:

$$\sigma_{\Sigma^0 p\to\Lambda p}=\left(\frac{p_\Lambda^{\rm cm}}{p_\Sigma^{\rm cm}}\right)^2\sigma_{\Lambda p\to\Sigma^0 p}(p'_\Lambda), \tag{77}$$

where the quantities $\sigma_{\Lambda p\to\Sigma^0 p}$, $p_\Lambda^{\rm cm}$ and $p_\Sigma^{\rm cm}$ are defined above by Eqs. (44), (45), in which one has to put:

$$\begin{aligned} s_\Sigma &= (E_{\Sigma^0}+m_N)^2-p_{\Sigma^0}^2, p'_\Lambda=\sqrt{E'^2_\Lambda-(<m_\Lambda^*>)^2},\\ E'_\Lambda &= [s_\Sigma-m_N^2-(<m_\Lambda^*>)^2]/(2m_N). \end{aligned} \tag{78}$$

For the second cross section in Eq. (76) we adopt the following parametrization, suggested in Ref. [62]:

$$\sigma_{\Sigma^0 p\to\Sigma^+ n}(p_{\Sigma^0})=22.4/p_{\Sigma^0}-1.08\ [\rm mb], \tag{79}$$

where the Σ^0 momentum p_{Σ^0} is measured in GeV/c.

The differential cross section for Λ hyperon production in pA collisions in coincidence with the K^+ meson from the two-step processes (48)–(50) and (70)–(72), corresponding to the kinematical conditions of the ANKE experiment, can be defined analogously to Eq. (46) as:

$$\begin{aligned} &\left\langle\frac{{\rm d}\sigma_{\rm pA\to\Lambda X}^{\rm (sec)}(\boldsymbol{p}_0,p_\Lambda)}{{\rm d}p_\Lambda{\rm d}\boldsymbol{\Omega}_\Lambda}\right\rangle_{\Delta\boldsymbol{\Omega}_\Lambda\Delta\boldsymbol{p}_{\rm K^+}}=\frac{1}{(2\pi)(1-\cos 6^\circ)}\\ &\times\int\limits_{0.2\ {\rm GeV}/c}^{0.6\ {\rm GeV}/c}{\rm d}p_{\rm K^+}\int\limits_{\cos 12^\circ}^{1}{\rm d}\cos\theta_{\rm K^+}\int\limits_{\cos 6^\circ}^{1}{\rm d}\cos\theta_\Lambda\int\limits_0^{2\pi}{\rm d}\phi_{\rm K^+}\int\limits_0^{2\pi}{\rm d}\phi_\Lambda\\ &\times\left[\frac{{\rm d}\sigma_{\rm pA\to\Lambda K^+X}^{\rm (sec),(\pi)}(\boldsymbol{p}_0,\boldsymbol{p}_\Lambda,\boldsymbol{p}_{\rm K^+})}{{\rm d}\boldsymbol{p}_\Lambda{\rm d}\boldsymbol{p}_{\rm K^+}}+\frac{{\rm d}\sigma_{\rm pA\to\Lambda K^+X}^{\rm (sec),(\Sigma^0)}(\boldsymbol{p}_0,\boldsymbol{p}_\Lambda,\boldsymbol{p}_{\rm K^+})}{{\rm d}\boldsymbol{p}_\Lambda{\rm d}\boldsymbol{p}_{\rm K^+}}\right]\\ &\times p_\Lambda^2 p_{\rm K^+}^2. \end{aligned} \tag{80}$$

We now discuss the results of calculations within the approach outlined above.

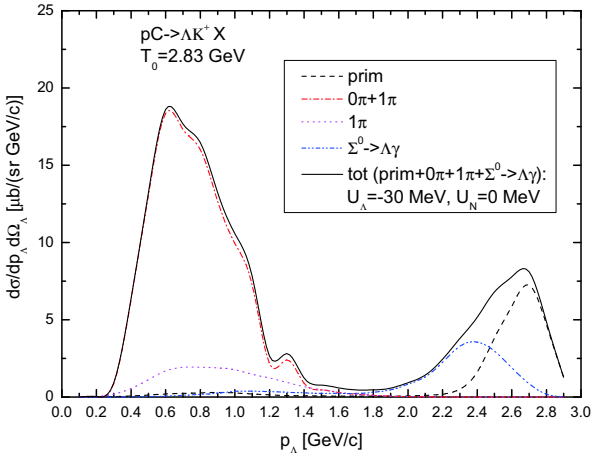

Fig. 5. (color online) Differential cross section for the production of Λ hyperons in coincidence with K^+ mesons from primary (1)–(6) (dashed line), secondary (49), (50) (dotted-dashed line), secondary (50) (dotted line), secondary (72) (dot-dot-dashed line) and primary (1)–(6) plus secondary (49), (50), (72) (solid line) channels in the ANKE acceptance window as a function of lambda momentum in the interaction of protons of energy of 2.83 GeV with C target nucleus for Λ effective scalar potential depth $U_\Lambda=-30$ MeV.

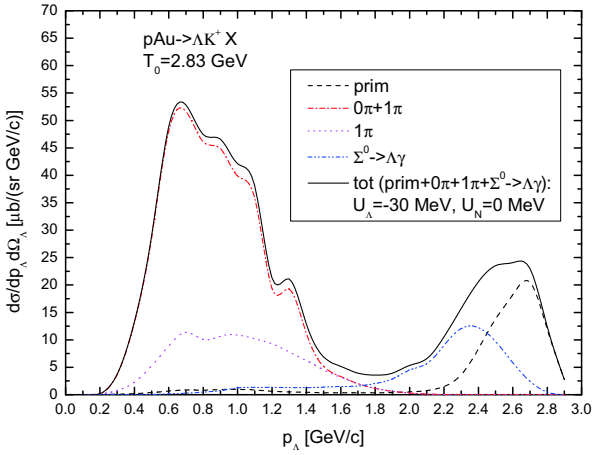

Fig. 6. (color online) Differential cross section for the production of Λ hyperons in coincidence with K^+ mesons from primary (1)–(6) (dashed line), secondary (49), (50) (dotted-dashed line), secondary (50) (dotted line), secondary (72) (dot-dot-dashed line) and primary (1)–(6) plus secondary (49), (50), (72) (solid line) channels in the ANKE acceptance window as a function of lambda momentum in the interaction of protons of energy of 2.83 GeV with Au target nucleus for Λ effective scalar potential depth $U_\Lambda=-30$ MeV.

1) Using this cross section in Eq. (27), we assume that the quasi-elastic Σ^0 rescatterings on intranuclear nucleons do not lead to the loss of Σ^0 hyperons, which may undergo subsequently $\Sigma^0\to\Lambda\gamma$ decays.

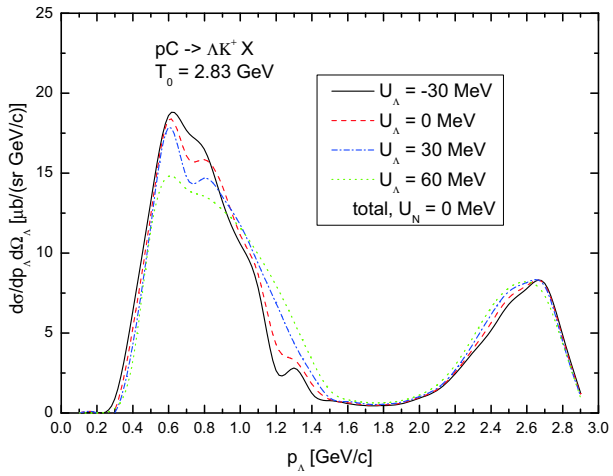

Fig. 7. (color online) Differential cross section for the production of Λ hyperons in coincidence with the K^+ mesons from primary plus secondary channels in the ANKE acceptance window as a function of lambda momentum in the interaction of protons of energy of 2.83 GeV with C target nucleus for effective scalar Λ potentials at saturation density $U_\Lambda = -30$ MeV (solid line), $U_\Lambda = 0$ MeV (dashed line), $U_\Lambda = 30$ MeV (dotted-dashed line) and $U_\Lambda = 60$ MeV (dotted line).

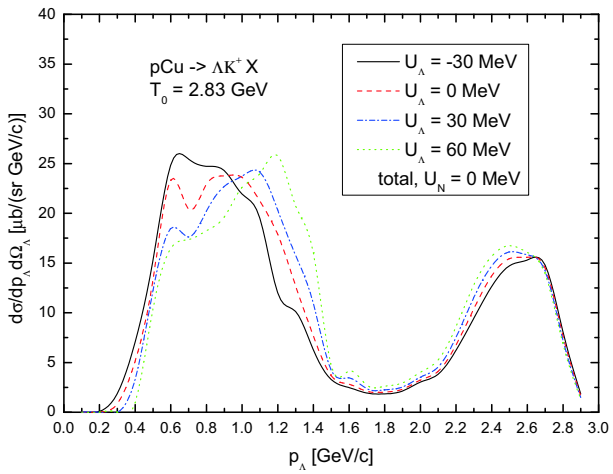

Fig. 8. (color online) Differential cross section for the production of Λ hyperons in coincidence with the K^+ mesons from primary plus secondary channels in the ANKE acceptance window as a function of lambda momentum in the interaction of protons of energy of 2.83 GeV with Cu target nucleus for effective scalar Λ potentials at saturation density $U_\Lambda = -30$ MeV (solid line), $U_\Lambda = 0$ MeV (dashed line), $U_\Lambda = 30$ MeV (dotted-dashed line) and $U_\Lambda = 60$ MeV (dotted line).

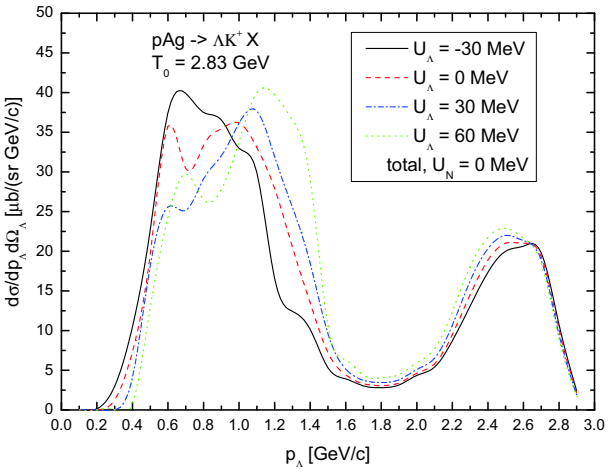

Fig. 9. (color online) Differential cross section for the production of Λ hyperons in coincidence with the K^+ mesons from primary plus secondary channels in the ANKE acceptance window as a function of lambda momentum in the interaction of protons of energy of 2.83 GeV with Ag target nucleus for effective scalar Λ potentials at saturation density $U_\Lambda = -30$ MeV (solid line), $U_\Lambda = 0$ MeV (dashed line), $U_\Lambda = 30$ MeV (dotted-dashed line) and $U_\Lambda = 60$ MeV (dotted line).

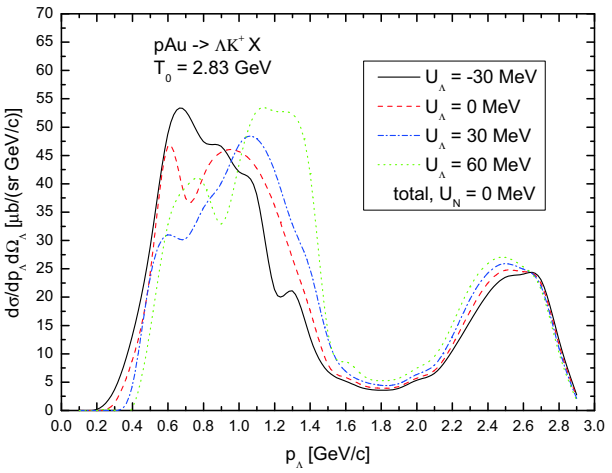

Fig. 10. (color online) Differential cross section for the production of Λ hyperons in coincidence with the K^+ mesons from primary plus secondary channels in the ANKE acceptance window as a function of lambda momentum in the interaction of protons of energy of 2.83 GeV with Au target nucleus for effective scalar Λ potentials at saturation density $U_\Lambda = -30$ MeV (solid line), $U_\Lambda = 0$ MeV (dashed line), $U_\Lambda = 30$ MeV (dotted-dashed line) and $U_\Lambda = 60$ MeV (dotted line).

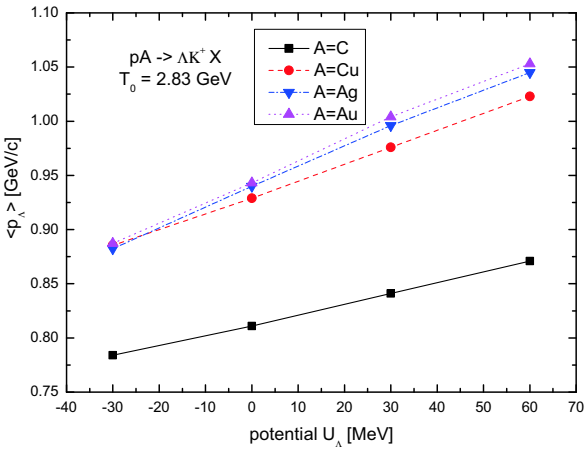

Fig. 11. (color online) Average momenta of Λ hyperons in the low-momentum parts of their spectra, shown in Figs. 7–10, from pC, pCu, pAg and pAu interactions at an incident energy of 2.83 GeV as functions of the effective scalar Λ potential U_Λ at normal nuclear density. The lines are to guide the eye.

3 Results

First, we consider the differential Λ production cross sections in the ANKE acceptance window from the one-step, two-step and one- plus two-step creation mechanisms in pC and pAu reactions at 2.83 GeV beam energy, calculated on the basis of Eqs. (46) and (80), in the scenario for the Λ effective scalar potential depth $U_\Lambda = -30$ MeV. These cross sections are presented in Figs. 5 and 6, respectively. The secondary ΛK^+ production processes (49), (50) with a pion in an intermediate state are important compared to the primary processes (1)–(6) and the secondary process (72) associated with the production of Λs via the vacuum decay of intermediate Σ^0 hyperons, in the chosen kinematics at laboratory lambda momenta $\leqslant$ 1.8 GeV/c, for both target nuclei. The dominance here is substantially more pronounced for the $\pi N \to \Lambda K^+$ channels. At higher Λ momenta around 2.4 and 2.7 GeV/c, however, the two-step with intermediate Σ^0 hyperons and one-step creation mechanisms are, respectively, dominant. Evidently, the dependence of the considered coincident Λ spectrum on the Λ effective scalar potential should exist mainly at low lambda momenta (cf. Figs. 7–10). This means that the secondary pion–nucleon production processes have to be accounted for in the analysis of the data on ΛK^+ pair creation in pA collisions obtained in the ANKE experiment with the aim of extracting the Λ–nuclear potential. The relative roles of the individual ΛK^+ production channels for other considered options for this potential at saturation density and target nuclei are similar to those, illustrated in Figs. 5 and 6 for a depth $U_\Lambda = -30$ MeV for C and Au targets. It is clearly seen from Figs. 5 and 6 that the two-bump structure in the results (and in those shown in Figs. 7–10) is mainly caused by the two-step (lower bump) and one-step (higher bump) ΛK^+ production mechanisms.

In Figs. 7–10 we show the results of our calculations following Eqs. (46) and (80) for the overall differential cross sections for the production of Λ hyperons in coincidence with the K^+ mesons on C, Cu, Ag and Au target nuclei in the kinematical conditions of the ANKE experiment. These were obtained for the incident energy of 2.83 GeV, considering four options for the effective scalar hyperon potential U_Λ at normal nuclear matter density, as indicated in the insets. These cross sections are appreciably sensitive to the Λ potential at momenta less than 1.8 GeV/c for all target nuclei considered; namely, their strengths shift to higher momenta with increasing Λ potential U_Λ up to 60 MeV. The sensitivity of the strength of the low-momentum part of the Λ spectrum on the scalar Λ potential U_Λ, shown in Figs. (7)–(10), can be exploited to infer the momentum dependence of this potential from the direct comparison of the shapes of the calculated Λ hyperon differential distributions with that determined in the ANKE experiment by putting the data in Λ momentum bins. As a less differential and an additional measure for the correlation between the above strength and the Λ–nuclear potential U_Λ, one can use the average momentum $<p_\Lambda>$, defined as

$$<p_\Lambda> = \int\limits_{0.1\ \mathrm{GeV}/c}^{1.8\ \mathrm{GeV}/c} \frac{p_\Lambda \mathrm{d}p_\Lambda \mathrm{d}\sigma}{\mathrm{d}p_\Lambda \mathrm{d}\boldsymbol{\Omega}_\Lambda} \Bigg/ \int\limits_{0.1\ \mathrm{GeV}/c}^{1.8\ \mathrm{GeV}/c} \frac{\mathrm{d}p_\Lambda \mathrm{d}\sigma}{\mathrm{d}p_\Lambda \mathrm{d}\boldsymbol{\Omega}_\Lambda},$$

where $\mathrm{d}\sigma/\mathrm{d}p_\Lambda \mathrm{d}\boldsymbol{\Omega}_\Lambda$ are the Λ differential cross sections presented in Figs. 7–10. The use of this quantity has the advantage of significantly decreasing the uncertainties of absolute normalization of both the model calculations and the experimental data. The average momentum $<p_\Lambda>$ as a function of potential U_Λ is plotted in Fig. 11. It is seen that the carbon nucleus is not optimal for determining this potential. The heavy silver and gold target nuclei show the highest sensitivity to it. Thus, for example, for the gold nucleus the difference between the mean momenta $<p_\Lambda>$ corresponding to the Λ potential at saturation density $U_\Lambda = -30$ MeV and $U_\Lambda = 60$ MeV, is 166 MeV/c, whereas the same difference for the carbon target nucleus is only 87 MeV/c[1)]. Therefore, a comparison of the above results with the experimentally deter-

1) The analogous difference between the average momenta corresponding to the high-momentum region of 1.8–2.9 GeV/c of the Λ spectrum of the Au nucleus, as well as to the same potentials $U_\Lambda = -30$ MeV and $U_\Lambda = 60$ MeV, amounts, as our calculations show, to 42 MeV/c. This demonstrates the very moderate sensitivity of the considered momentum distributions to the adopted Λ in-medium modification scenarios at high momenta of interest also.

mined average momentum in the low-momentum part of the Λ spectrum of the heavy target nuclei under consideration will also allow one to deduce the effective scalar potential U_Λ in cold nuclear matter at this momentum[1)]. Knowing this potential and using Eqs. (19) and (20), we can easily recover the single-particle potential $V^{\rm SEP}_{\Lambda A}$ at saturation density for in-medium momentum p'_Λ, corresponding to the experimentally determined average momentum $< p_\Lambda >$. Such a data point may also help to discriminate between the existing models of the YN interaction at finite momenta.

Thus, we come to the conclusion that the coincident observables considered above can be useful to help determine the Λ–nucleus potential at finite momenta in the region $\leqslant$ 1.8 GeV/c, where the theoretical predictions for it are available.

4 Conclusions

In this paper we calculated the momentum dependences of the absolute differential cross sections for the production of Λ hyperons in coincidence with the K^+ mesons from pA (A=C, Cu, Ag, and Au) collisions at 2.83 GeV beam energy in the kinematical conditions of the ANKE experiment, performed at COSY, by considering incoherent primary proton–nucleon, secondary pion–nucleon ΛK^+ production processes and processes associated with the creation of intermediate $\Sigma^0 K^+$ pairs in the framework of a nuclear spectral function approach within the different scenarios for the Λ hyperon effective scalar potential. It was found that the shapes of the cross sections are appreciably sensitive to this potential at Λ momenta less than 1.8 GeV/c. This opens a good possibility to determine the above potential here from direct comparison of the results presented in this work with the data from the ANKE-at-COSY experiment. It was also demonstrated that the two-step pion–nucleon production channels dominate in the low-momentum ΛK^+ creation in the chosen kinematics and, hence, they should be taken into account in the analysis of these data with the purpose of getting definite information on the Λ nuclear potential at finite momenta.

The authors gratefully acknowledge A. Polyanskiy for his interest in this work.

References

1 A. Gal, E. V. Hungerford, and D. J. Millener, Rev. Mod. Phys., **88**: 035004 (2016)
2 M. Nekipelov et al, Phys. Lett. B, **540**: 207 (2002); G. Agakishiev et al, Phys. Rev. C, **82**: 044907 (2010)
3 M. Lutz, Phys. Lett. B, **426**: 12 (1998)
4 L. Tolos, A. Ramos, and E. Oset, Phys. Rev. C, **74**: 015203 (2006)
5 L. Tolos, D. Cabrera, and A. Ramos, Phys. Rev. C, **78**: 045205 (2008)
6 L. Tolos, A. Ramos, A. Polls, and T. T. S. Kuo, Nucl. Phys. A, **690**: 547 (2001); L. Tolos, A. Ramos, and A. Polls, Phys. Rev. C, **65**: 054907 (2002)
7 E. Friedman, A. Gal, J. Mares, and A. Cieply, Phys. Rev. C, **60**: 024314 (1999)
8 A. Sibirtsev and W. Cassing, arXiv: nucl-th/9909053; W. Scheinast et al, Phys. Rev. Lett., **96**: 072301 (2006); T. Kishimoto et al, Nucl. Phys. A, **827**: 321c (2009); H. W. Barz and L. Naumann, Phys. Rev. C, **68**: 041901(R) (2003)
9 Yu. T. Kiselev et al, Phys. Rev. C, **92**: 065201 (2015)
10 V. K. Magas et al, Phys. Rev. C, **71**: 065202 (2005); A. Polyanskiy et al, Phys. Lett. B, **695**: 74 (2011); M. Hartmann et al, Phys. Rev. C, **85**: 035206 (2012); T. Ishikawa et al, Phys. Lett. B, **608**: 215 (2005); M. H. Wood et al, Phys. Rev. Lett., **105**: 112301 (2010)
11 C. Fuchs, Prog. Part. Nucl. Phys., **56**: 1 (2006); C. Hartnack et al, Phys. Rep., **510**: 119 (2012); O. Buss et al, Phys. Rep., **512**: 1 (2012)
12 Z. Q. Feng, Nucl. Phys. A, **919**: 32 (2013); Z. Q. Feng, W. J. Xie, and G. M. Jin, Phys. Rev. C, **90**: 064604 (2014)
13 G. Bunce et al, Phys. Rev. Lett., **36**: 1113 (1976); K. Heller et al, Phys. Lett. B, **68**: 480 (1977); K. Heller et al, Phys. Rev. Lett., **41**: 607 (1978); F. Lomanno et al, Phys. Rev. Lett., **43**: 1905 (1979); F. Abe et al, Phys. Rev. Lett., **50**: 1102 (1983); A. M. Smith et al, Phys. Lett. B, **185**: 209 (1987); B. E. Bonner et al, Phys. Rev. D, **38**: 729 (1988); V. Fanti et al (NA48 Collaboration), Eur. Phys. J. C, **6**: 265 (1999); B. Lundberg et al, Phys. Rev. D, **40**: 3557 (1989)
14 G. Agakishiev et al, Eur. Phys. J. A, **50**: 81 (2014)
15 O. Hashimoto and H. Tamura, Prog. Part. Nucl. Phys., **57**: 279 (2010); A. Feliciello and T. Nagae, Rep. Prog. Phys., **78**: 096301 (2015)
16 M. Kaskulov and E. Oset, Phys. Rev. C, **73**: 045213 (2006)
17 M. Kaskulov, L. Roca, and E. Oset, Eur. Phys. J. A, **28**: 139 (2006); E. Ya. Paryev, Yad. Fiz., **75**: 1602 (2012)
18 M. F. M. Lutz, C. L. Copra, and M. Moeller, Nucl. Phys. A, **808**: 124 (2008)
19 D. Cabrera et al, Phys. Rev. C, **90**: 055207 (2014)
20 S. Petschauer et al, Eur. Phys. J. A, **52**: 15 (2016); Ulf-G. Meissner and J. Haidenbauer, arXiv: 1603.06429 [nucl-th]
21 V. Flaminio et al Compilation of cross–sections. III–p and $\bar{p}$ induced reactions. CERN-HERA **79−03** (1979)
22 J. Balewski et al (COSY-11 Collaboration), Nucl. Phys. A, **626**: 85c (1997)
23 J. T. Balewski et al (COSY-11 Collaboration), Phys. Lett. B, **420**: 211 (1998)
24 S. Sewerin et al (COSY-11 Collaboration), Phys. Rev. Lett., **83**: 682 (1999)
25 P. Kowina et al (COSY-11 Collaboration), Eur. Phys. J. A, **22**: 293 (2004)
26 R. Bilger et al (COSY-TOF Collaboration), Phys. Lett. B, **420**: 217 (1998)
27 S. Abd El-Samad et al (COSY-TOF Collaboration), Phys. Lett. B, **632**: 27 (2006); S. Abd El-Samad et al (COSY-TOF Collaboration), Phys. Lett. B, **688**: 142 (2010)
28 M. Abdel-Bary et al (COSY-TOF Collaboration), Eur. Phys. J. A, **46**: 27 (2010)
29 Yu. Valdau et al (ANKE Collaboration), Phys. Lett. B, **652**: 245 (2007); Yu. Valdau et al (ANKE Collaboration), Phys. Rev.

1) It should be noted that an analogous possibility was recently realized for the ω mesons in Ref. [70].

C, **81**: 045208 (2010)
30 J. Adamczewski-Musch et al (HADES Colaboration), Phys. Rev. C, **95**: 015207 (2017); arXiv: 1611.01040 [nucl-ex]
31 E. Ya. Paryev, Eur. Phys. J. A, **5**: 307 (1999)
32 G. Fäldt and C. Wilkin, Z. Phys. A, **357**: 241 (1997)
33 M. Nekipelov et al, J. Phys. G: Nucl. Part. Phys., **34**: 627 (2007)
34 G. Agakishiev et al, Phys. Rev. C, **90**: 015202 (2014); arXiv: 1403.6662 [nucl-ex]
35 G. Q. Li, C.-H. Lee, G. E. Brown, Nucl. Phys. A, **625**: 372 (1997)
36 G. Agakishiev et al, Phys. Rev. C, **90**: 054906 (2014); arXiv: 1404.7011 [nucl-ex]
37 Yu. Valdau et al (ANKE Collaboration), Phys. Rev. C, **84**: 055207 (2011)
38 M. Büscher et al, Eur. Phys. J. A, **22**: 301 (2004)
39 K. Tsushima et al, Phys. Rev. C, **59**: 369 (1999)
40 A. N. Ivanov et al, arXiv: nucl-th/0509055
41 G. Fäldt and C. Wilkin, Eur. Phys. J. A, **24**: 431 (2005)
42 E. Ya. Paryev, J. Phys. G: Nucl. Part. Phys., **40**: 025201 (2013)
43 H. Nagahiro, M. Takizawa, and S. Hirenzaki, Phys. Rev. C, **74**: 045203 (2006)
44 E. Ya. Paryev, Eur. Phys. J. A, **9**: 521 (2000)
45 K. Tsushima et al, Phys. Lett. B, **429**: 239 (1998)
46 C.-H. Lee et al, Phys. Lett. B, **412**: 235 (1997)
47 C. B. Dover and G. E. Walker, Phys. Rep., **89**: 1 (1982); D. J. Millener, C. B. Dover and A. Gal, Phys. Rev. C, **38**: 2700 (1988); Y. Yamamoto, H. Bando, and J. Zofka, Prog. Theor. Phys., **80**: 757 (1988)
48 M. Rufa et al, Phys. Rev. C, **42**: 2469 (1990)
49 N. K. Glendenning et al, Phys. Rev. C, **48**: 889 (1993)
50 Y. Yamamoto and H. Bando, Phys. Lett. B, **214**: 173 (1988)
51 J. Hu, E. Hiyama, and H. Toki, Phys. Rev. C, **90**: 014309 (2014)
52 M. Kohno and Y. Fujiwara, Phys. Rev. C, **79**: 054318 (2009); M. Kohno, Phys. Rev. C, **81**: 014003 (2010)
53 T. Inoue et al, arXiv: 1612.08399 [hep-lat]
54 G. Q. Li and C. M. Ko, Phys. Rev. C, **54**: 1897 (1996)
55 E. Ya. Paryev, Yad. Fiz., **71**: 1985 (2008)
56 E. Ya. Paryev, J. Phys. G: Nucl. Part. Phys., **43**: 015106 (2016)
57 E. Ya. Paryev, J. Phys. G: Nucl. Part. Phys., **37**: 105101 (2010)
58 E. Ya. Paryev, M. Hartmann, and Yu. T. Kiselev, J. Phys. G: Nucl. Part. Phys., **42**: 075107 (2015)
59 E. Ya. Paryev, J. Phys. G: Nucl. Part. Phys., **36**: 015103 (2009)
60 S. V. Efremov and E. Ya. Paryev, Eur. Phys. J. A, **1**: 99 (1998)
61 E. Ya. Paryev, Eur. Phys. J. A, **7**: 127 (2000)
62 S. K. Singh and M. J. Vicente Vacas, Phys. Rev. D, **74**: 053009 (2006)
63 J. Haidenbauer and Ulf-G. Meissner, Nucl. Phys. A, **936**: 29 (2015)
64 E. Friedman and A. Gal, Phys. Rep., **452**: 89 (2007)
65 J. Cugnon and R. M. Lombard, Nucl. Phys. A, **422**: 635 (1984)
66 A. Baldini et al, Landolt-Börnstein, New Series, **I/12a** (1988)
67 I. Zychor et al, Phys. Lett. B, **660**: 167 (2008)
68 E. Ya. Paryev, Phys. Atom. Nucl., **69**: 721 (2006)
69 A. V. Akindinov et al, J. Phys. G: Nucl. Part. Phys., **37**: 015107 (2010)
70 S. Friedrich et al, Phys. Lett. B, **736**: 26 (2014)